

Phosphorous-containing, amphiphilic ABB' copolymers as siRNA nanocarriers with enhanced stability, reduced in vitro cytotoxicity and efficient knockdown ability for treatment of ocular diseases

*Philipp Weingarten,<sup>a,†</sup> Molly Tzu-Yu Lin,<sup>b,†</sup> Moritz Kränzlein,<sup>a</sup> Agnes Fietz,<sup>b</sup> Iris Kachel,<sup>c</sup> José Hurst,<sup>b</sup> Sven Schnichels,<sup>b</sup> Friederike Adams,<sup>b,c\*</sup>*

**Supporting Information**

## 1) Materials and Methods

### General Information

All reactions were carried out under argon atmosphere using standard Schlenk techniques or in an Argon-filled glovebox. All glassware was heat dried under vacuum prior to use. Polymerizations with moisture and air-sensitive reactants were carried out in a MBraun LabMaster120 glovebox filled with argon 4.6 from Westfalen or using standard Schlenk techniques. Unless otherwise stated, all chemicals were purchased from Sigma-Aldrich or TCI and used as received. Toluene for polymerization reactions was dried using a MBraun SPS-800 solvent purification system and stored over 3 Å molecular sieve. The precursor complex  $\text{Cp}_2\text{Y}(\text{CH}_2\text{TMS})(\text{thf})$  was prepared according to literature procedures.<sup>1</sup> Diethyl vinylphosphonate (DEVP) and diallyl vinylphosphonate (DAIVP) were synthesized according to literature procedures, dried over calcium hydride and distilled prior to use.<sup>2,3</sup> 2-Vinylpyridine was dried over calcium hydride and distilled prior to use. Hyperbranched poly(ethylenimine) (PEI) was obtained from BASF (Ludwigshafen, DE, Lupasol WF, PEI,  $M_w = 25$  kDa, primary:secondary:tertiary amines 1:1.1:0.7) or from Sigma-Aldrich ( $M_n = 10$  kDa,  $M_w = 25$  kDa). Solvents for polymerization were used in an anhydrous form unless otherwise stated. As negative control siRNA either scrambled siRNA (5' - pCGUUAUCGCGUAUAAUACGCGUat, 3' - CAGCAAUUAGCGCAUAAUUAUGCGCAUAp) from Integrated DNA Technologies (Coralville, IA, USA) (indication of modified nucleotides: “p” denotes a phosphate residue, lower case letters are 2'-deoxyribonucleotides, capital letters are ribonucleotides, and underlined capital letters are 2'-O-methylribonucleotides) or Silencer<sup>TM</sup> negative control siRNA (Thermo Fisher Scientific, Darmstadt, Germany) was used.

### NMR Spectroscopy

NMR spectra were recorded on a Bruker AVIII-400 or an Avance III HD Bruker BioSpin 400 spectrometer at Technical University of Munich at the respective NMR facility. Unless otherwise stated, <sup>1</sup>H- and <sup>13</sup>C-NMR spectroscopic chemical shifts  $\delta$  are reported in ppm.  $\delta$  (<sup>1</sup>H) is calibrated to the residual proton signal of the deuterated solvent,  $\delta$  (<sup>13</sup>C) to the carbon signal of the solvent. Deuterated solvents were obtained from Sigma-Aldrich.

## Size-exclusion chromatography (SEC)

Absolute molecular weights and polydispersities of the polymers were determined via size-exclusion chromatography (SEC) with a sample concentration of 2 mg mL<sup>-1</sup>. Measurements of P2VP and the obtained block copolymers were performed on an Agilent PL-GPC 50 (Santa Clara, CA, USA) with an integrated RI unit, two light scattering detectors (15° and 90°), and a differential pressure viscosimeter with two Agilent PolarGel M columns. As eluent N,N-dimethylformamide (with 2.096 g L<sup>-1</sup> lithium bromide added) at 30 °C was used. Absolute molecular weights of P2VP were determined using  $dn/dc = 0.149 \text{ mL g}^{-1}$  from the literature. Size-exclusion chromatography multi-angle light scattering (SEC-MALS) was used to determine polydispersity of polymer AB-4 ( $c = 2 \text{ mg mL}^{-1}$ ) with a Wyatt Dawn Heleos II MALS light scattering unit and a Wyatt Optilab rEX 536 RI unit in THF:H<sub>2</sub>O = 1:1 (with 9 g L<sup>-1</sup> *tetra-n*-butyl-ammonium bromide and 272 mg L<sup>-1</sup> 2,6-di-*tert*-butyl-4-methylphenol added) as eluent at 40 °C on two Agilent PolarGel-M columns.

## Dialysis

Purification of products via dialysis was performed with *Spectra/Por 1* dialysis membranes (regenerated cellulose) from *Spectrum*<sup>TM</sup> against deionized water. The molecular weight cut-off (MWCO) of the membranes was 6-8 kDa, and a 3.3 mL cm<sup>-1</sup> volume-length ratio was used.

## Lyophilization

The polymer samples subject to freeze-drying were dissolved in either ultrapure water or 1,4-dioxane and frozen under constant rotation in liquid nitrogen. For lyophilization, a VaCo 5-II-D from Zirbus Technology GmbH was used, and the pressure was adjusted to 2 mbar with a condenser temperature of -90 °C.

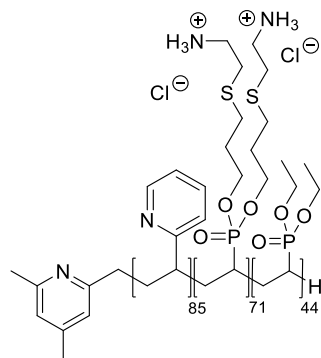
## Preparation of Polyplexes<sup>4</sup>

Polymer-siRNA complexes (polyplexes) were prepared in aqueous stock solutions and diluted with 10 mM freshly filtered HEPES buffer (pH 7.2) to predetermined concentrations. A defined amount of siRNA was added in a microcentrifuge tube to obtain polyplexes at various N/P ratios

that were incubated for 20 min. The N/P ratio is defined as the molar ratio between polymer amine groups (N) and siRNA phosphate groups (P). The amount of polymer needed to obtain different N/P ratios was calculated according to the following equation:

$$m_{\text{polymer}} [\text{mg}] = n_{\text{siRNA}} [\text{mmol}] \cdot M_{\text{protonable unit}} [\text{g mol}^{-1}] \cdot \text{N/P} \cdot N_{\text{nucleotides siRNA}}$$

The protonable unit of each polymer was determined by dividing its molar mass by the number of protonable primary amines present in each polymer (2-fold for each DAIVP monomer). As discussed, the pyridyl units do not contribute to siRNA encapsulation, which allows to not take them into account in this calculation. In terms of hyperbranched PEI 25 kDa, all aliphatic amines are considered when calculating the N/P ratio ( $M_{\text{protonable unit}} = 43 \text{ g mol}^{-1}$ ).



Example: ABB'-1  
 $M_n = 45700 \text{ g mol}^{-1}$   
 $M_{\text{protonable unit}} = 322 \text{ g mol}^{-1}$

Polymer	Protonable unit
AB-1	$334 \text{ g mol}^{-1}$
AB-2	$256 \text{ g mol}^{-1}$
ABB'-1	$322 \text{ g mol}^{-1}$
ABB'-2	$629 \text{ g mol}^{-1}$
ABB'-3	$493 \text{ g mol}^{-1}$
ABB'-4	$690 \text{ g mol}^{-1}$

### siRNA Encapsulation Assay by SYBR Gold Assay

Polyplexes were prepared according to the described procedure at various N/P ratios. 4X SYBR Gold solution (30  $\mu\text{L}$ ) was added to each well, and the plate was incubated for 10 min in the dark. The fluorescence signal was determined by using a fluorescence plate reader (Tecan Spark, Tecan Trading AG, Switzerland) at 485 nm and 535 nm excitation and emission wavelengths, respectively. An analogous procedure with free siRNA was used as 100% value. Measurements were performed as triplicate, and the results are shown as mean values ( $n = 3$ ). A SYBR Gold

assay was used to determine the capacity of the polymers to condense siRNA according to a procedure previously described.<sup>5</sup> Polyplexes with 50 pmol of siRNA were prepared in HEPES buffer, and 100  $\mu\text{L}$  of each polyplex solution was distributed in a white FluoroNunc 96-well plate (FisherScientific, Hampton, NH, USA).

### **Dynamic Light Scattering (DLS)**

The particle size, polydispersity index (PDI), and zeta potential of aqueous polymer solutions ( $2.5 \text{ mg mL}^{-1}$ ) were measured using a Zetasizer Ultra Red (Malvern Instruments, Malvern, UK) using a disposable sizing cuvette (DTS0012) at a backscattering collection angle. Samples were equilibrated at  $25^\circ\text{C}$  for 120 s and all settings were left automatic. Sizes were measured three times and averaged. Micelles formed under aqueous conditions were filtered prior to DLS and zeta potential measurements (PURADISC 25 AS Disposable Filter DEVICE or PES syringe filter with  $0.45 \mu\text{m}$ ). Polyplexes were formed in HEPES buffer and were measured using a Zetasizer Nano ZS (Malvern Instruments, Malvern, UK) at a backscattering collection running 15 scans three times per sample or using a Zetasizer Ultra Red (Malvern Instruments, Malvern, UK). A total volume of  $100 \mu\text{L}$  of each sample was used. Zeta potentials were measured using a Zeta Cell (Zetasizer Nano series, Malvern, UK) containing a 7X dilution of another  $100 \mu\text{L}$  sample aliquot by laser Doppler anemometry (LDA) or by electrophoretic light scattering (ELS), with each run consisting of 30 scans. Results are presented as z-average  $\pm$  standard deviation ( $n = 3$ ), polydispersity and zeta potentials  $\pm$  standard deviation ( $n = 3$ ).

### **Critical Micelle Concentration (CMC)**

The CMC measurements were conducted by following a procedure known from literature using Nile Red as the indicating dye for micelle formation.<sup>6</sup> Nile Red stock solution was prepared by dissolving the dye in DMSO to a concentration of  $0.8 \text{ mg mL}^{-1}$ . Concentrated stock solutions of each polymer were prepared in highly purified water, then combined with dye solution and additional HPW to provide the appropriate final concentrations. The solutions were sonicated for 30 min at  $35^\circ\text{C}$  then incubated at room temperature for 5 h. Afterward, the solutions were transferred to a 96-well microplate and allowed to equilibrate at  $25^\circ\text{C}$  for 10 min. All fluorescence

measurements were carried out using a fluorescence plate reader (Tecan Spark, Tecan Trading AG, Switzerland) at 485 nm and 636 nm excitation and emission wavelengths, respectively. Fluorescence intensity was plotted as a function of surfactant concentration, and each CMC value was calculated as follows: Two linear regions were determined and both fitted by linear regression. The concentration at which these lines intersect was calculated and determined to be the CMC.

### **Titration experiments**

Acid-base titration studies over pH values ranging from 12 to 2 were performed to determine the buffering capacity of the studied polymers. In brief, an aqueous polymer solution with a concentration of  $1 \text{ mg mL}^{-1}$  was prepared, and the pH was adjusted to 11.0 with 0.1 M NaOH. Subsequently, the solution was titrated with 0.05 M HCl, and pH change was measured after every 50  $\mu\text{L}$  addition until the pH of the polymer solutions decreased to a pH of 3. The pH value was monitored with a pH meter and an electrode at 25 °C (SI Analytics TitroLine® 7000, SI Analytics, Mainz).

### **Cultivation of MIO-M1 cell line**

The human Müller cell line Moorfields/Institute of Ophthalmology-Müller 1 (MIO-M1) was obtained from the UCL Institute of Ophthalmology, London, UK.<sup>7</sup> MIO-M1 cells were cultivated in MIO-M1 culture medium containing high-glucose DMEM (Thermo Fisher Scientific, Karlsruhe, Germany) supplemented with 10% FBS and 1% penicillin/streptomycin (P/S, Gibco, Germany) at 37°C with 5% CO<sub>2</sub>.

### ***In vitro* cell viability assay**

To evaluate the cytotoxic effects of the synthesized polymers, the effect of polymers on cellular mitochondrial activity and cell density were investigated using MTS assay and crystal violet staining, respectively.<sup>8,9</sup> A total of 10,000 MIO-M1 cells (p42-p45) were seeded in a transparent 96-well plate for 17h to achieve 80-90% confluency. After 24 hours, the cell medium was removed and each well was treated with 100  $\mu\text{L}$  of different concentrations of polymers (5, 15, 25, 100, 150, 250, 500, 750  $\mu\text{g mL}^{-1}$ ) prepared in prewarmed high glucose ( $4.5 \text{ g L}^{-1}$ ) DMEM medium

(Thermo Fisher Scientific, Darmstadt, Germany) supplemented with 10% fetal bovine serum (FBS, Thermo Fisher Scientific, Darmstadt, Germany) and 1% penicillin/streptomycin (P/S; Gibco, Germany). Following 24 hours of treatment at 37°C and 5% CO<sub>2</sub>, MTS assay was carried out to evaluate metabolic activity of the treated cells according to the manufacture's instruction. Briefly, 20 µL of the CellTiter 96 ® Aqueous One Solution Reagent (Promega Corporation, Madison, WI, USA) was added directly into each well and incubated for 90 minutes at 37°C. Subsequently, the absorbance was measured at 490 nm with reference wavelength set at 690 nm for background correction using a Tecan Reader (NanoQuant Infinite M200). After MTS analysis, medium was removed and the cells were fixed with 4% PFA (paraformaldehyde, Merck, Darmstadt, Germany) for 15 minutes at room temperature (RT). Upon cell fixation, cells were washed with milliQ water before staining with crystal violet solution (Merck KGaA, Darmstadt, Germany) for 30 minutes. The crystal violet-stained samples were washed for four times with MilliQ water, followed by 1% sodium dodecyl sulfate (SDS, AppliChem, Darmstadt, Germany) treatment for 1h at RT. The absorbance was measured at 595 nm using the Tecan Reader. All data is shown as mean ± standard deviation from five replicates after normalizing to the untreated control wells representing 100% mitochondrial activity and 100% cell number for MTS assay and crystal violet staining, respectively.

### **Calcein assay**

Calcein is a membrane-impermeable fluorescent dye that can be used to assess the capability of endosomal escape upon endocytosis of the tested polymers.<sup>10</sup> To assess the capability of endosomal escape of polymer/siRNA polyplex for potential nucleic acid delivery, a total of 50,000 MIO-M1 cells were seeded per well in a 24-well plate one day prior to the assay procedure. Polymer/siRNA complexes were prepared at N/P 2.0 and 5.0 in 10 mM HEPES buffer using Silencer™ negative control siRNA (Thermo Fisher Scientific, Darmstadt, Germany). Following the polyplex formation for 15 minutes at RT, the polyplex solution was added into the respective wells containing medium supplemented with calcein (Tokyo Chemical Industry Co., LTD, Tokyo, Japan) at the final concentration of 150 µg mL<sup>-1</sup>. Two media: Opti-MEM™ (Thermo Fisher Scientific, Darmstadt, Germany) and normal medium (high glucose DMEM containing 10% FBS without antibiotics; NM) were used to evaluate the optimal condition for the downstream

experiment on *in vitro* RNAi intervention. After 4h incubation at 37°C with 5% CO<sub>2</sub>, cells were washed, counterstained with Hoechst dye for nuclei, and imaged using a fluorescent microscope (AXIO Observer, Zeiss, Germany) with a GFP filter set.

### **RELA/NFκB (p65) gene silencing in MIO-M1 cell line**

A total of 50,000 MIO-M1 (p36-40) was seeded in 24-well plates in DMEM/F-12 medium supplemented with 10% FBS without antibiotics. After 17-24h, MIO-M1 were transfected with AB-2/siRNA, ABB'-1/siRNA, and ABB'-2/siRNA polyplexes at N/P 5.0 encapsulating 50 pmol commercially available siRNA against RELA proto-oncogene, NFκB subunit (p65; Ambion™, Darmstadt, Germany). As a positive control, MIO-M1 cells were transfected with lipoplexes using Lipofectamine™ RNAiMAX Transfection Reagent (Thermo Fisher Scientific, Darmstadt, Germany) with the same amount of siNFκB (p65). A universal negative control siRNA (Silencer™ Negative Control No. 1 siRNA; ThermoFisher Scientific) was employed as negative control (siNC) for non-specific gene inhibition of the siRNA used in this study. An additional control with cells treated with either only siNC or siNFκB (p65) was included to highlight the effect of cationic polymers in polymer/siRNA transfection. The untreated MIO-M1 cells (untreated control; UC) served as an internal control as reference. The polymer/siRNA transfected cells were incubated for 72 h at 37°C, 5% CO<sub>2</sub> for subsequent western blot analysis.

### **Western blot and densitometric analysis**

To isolate the proteins for western blot analysis, the polymer/siRNA transfected MIO-M1 cells were first trypsinized using Trypsin/EDTA (0.25%, Thermo Fisher Scientific, Darmstadt, Germany), followed by centrifugation to obtain the cell pellets. The samples were homogenized in a cell extraction buffer (Thermo Fisher Scientific, Darmstadt, Germany) containing 1 mM PMSF and protease inhibitor cocktail set III, EDTA free (Cat no.: 359134, Calbiochem, San Diego, CA, USA) on ice prior to cell lysate collection upon centrifugation step at 13,000 rpm for 10 minutes at 4°C. A 10% Mini-PROTEAN TGX Precast Gel (Bio-rad, Feldkirchen, Germany) was used according to manufacturer's protocol. Briefly, 10 µg protein was loaded with a total volume of 15 µl per lane (containing 1x Laemmli Buffer, Bio-rad, Feldkirchen, Germany) and the samples

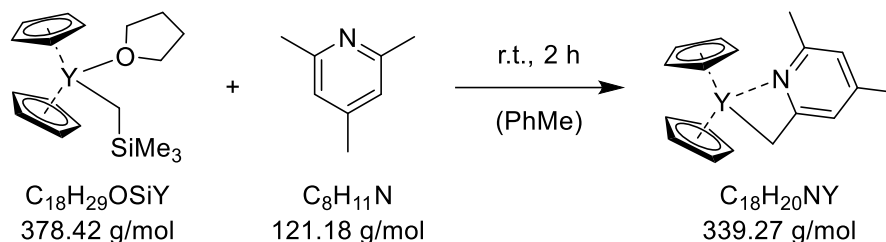
were subjected to RELA/NF- $\kappa$ B (p65) and housekeeping  $\beta$ -actin as loading control (Table S3). Corresponding secondary antibody IRDye 800 RD goat anti-mouse against RELA/NF- $\kappa$ B (p65) and IRDye 680 RD goat anti-rabbit against  $\beta$ -Actin were used to visualize protein bands. All antibodies were diluted in EveryBlot Blocking buffer containing 0.05% Tween-20. Proteins were detected at 700 and 800 nm, and the quantification analysis was evaluated using an Odyssey infrared imager system 2.1 (LI-COR Bioscience). The signal intensity of RELA/NF- $\kappa$ B (65) appeared at 65 kDa was normalized to its corresponding  $\beta$ -actin (42 kDa) signal intensities. The obtained results were then further normalized to untreated control samples set as 100% for analysis. Further densitometric analysis was performed using three independent experiments. All data represents mean  $\pm$  standard deviation.

### **Statistical analysis**

One-way ANOVA with Bonferroni mean comparison was used in the statistical analysis of densitometric results. A  $p > 0.12$  is considered not significant (ns);  $*p \leq 0.03$ ,  $**p \leq 0.002$  and  $***p < 0.001$  is considered significantly different. All data represent mean  $\pm$  standard deviation from  $n=3$  replicates.

## 2) Polymerization Procedures and Characterization

### *In situ* CH-bond activation of $\text{Cp}_2\text{Y}(\text{CH}_2\text{TMS})(\text{thf})$ with *sym*-collidine



$\text{Cp}_2\text{Y}(\text{CH}_2\text{TMS})(\text{thf})$  (5.11 mg, 13.5  $\mu\text{mol}$ , 1.0 eq.) was dissolved in 4 mL toluene, and 1.64 mg *sym*-collidine (13.5  $\mu\text{mol}$ , 1.0 eq.) was added. The solution immediately turned yellow. After 2 h, full conversion was observed via  $^1\text{H-NMR}$  spectroscopy.

$^1\text{H-NMR}$  (400 MHz,  $\text{C}_6\text{D}_6$ , 300 K):  $\delta$  (ppm) = 6.40 (s, 1 H,  $\text{H}_{\text{Ar,sym-col}}$ ), 6.04 (s, 10  $\text{H}_{\text{Cp}}$ ), 5.83 (s, 1 H,  $\text{H}_{\text{Ar,sym-col}}$ ), 2.32 (s, 2 H,  $\text{CH}_2$ ), 1.94 (s, 3 H,  $\text{CH}_3$ ), 1.86 (s, 3 H,  $\text{CH}_3$ ).

### General P2VP-*b*-PDAIVP Copolymerization Procedure

After full conversion of the CH-bond activation, the respective equivalents of 2-vinylpyridine were added in one portion. The reaction mixture was stirred overnight. One aliquot (0.1 mL) was taken and subsequently quenched by addition of 0.4 mL wet  $\text{CD}_3\text{OD}$  (calculation of conversion via  $^1\text{H-NMR}$  spectroscopy) while simultaneously the calculated amount of DAIVP was added to the reaction solution. After 2 h, an aliquot (0.1 mL) was taken from the reaction mixture and subsequently quenched with 0.1 mL wet  $\text{CD}_3\text{OD}$  (calculation of conversion via  $^{31}\text{P-NMR}$  spectroscopy). The reaction mixture was then quenched by the addition of 0.5 mL EtOH and subsequently precipitated from pentane (50 mL). After centrifugation, the liquid phase was decanted off. The polymer was dissolved in 1,4-dioxane and lyophilized overnight. The product was obtained as a colorless solid. Each aliquot was used for SEC analysis of the A- and AB-polymer, respectively.

$^1\text{H-NMR}$  (400 MHz, MeOD, 300 K):  $\delta$  (ppm) = 8.47-7.98 (m,  $\text{H}_{\text{Ar,P2VP}}$ ), 7.55-7.22 (m,  $\text{H}_{\text{Ar,P2VP}}$ ), 7.20-6.77 (m,  $\text{H}_{\text{Ar,P2VP}}$ ), 6.24-6.62 (m,  $\text{H}_{\text{Ar,P2VP}}$ ), 6.03 (br s,  $\text{H}_{\text{Allyl}}$ ), 5.40 (d,  $^3J = 17.2$  Hz,  $\text{H}_{\text{Allyl}}$ ), 5.31-5.20 (m,  $\text{H}_{\text{Allyl}}$ ), 4.62 (br s,  $\text{H}_{\text{CH}_2,\text{PDAIVP}}$ ), 2.97-1.30 (m,  $\text{H}_{\text{Vinylphosphonate backbone}}$ ), 2.00-1.50 (m,  $\text{H}_{\text{P2VP,backbone}}$ ).

**<sup>31</sup>P-NMR** (162 MHz, MeOD, 300 K):  $\delta$  (ppm) = 33.0 (br s).

The obtained intensities of the monomers vary due to the composition of the respective polymer.

### **General P2VP-*b*-(PDAIVP-*st*-PDEVV) Copolymerization Procedure**

After full conversion of the CH-bond activation was observed via <sup>1</sup>H-NMR spectroscopy, the respective equivalents of 2-vinylpyridine were added in one portion. The reaction mixture was stirred overnight. One aliquot (0.1 mL) was taken and subsequently quenched by addition of 0.4 mL wet CD<sub>3</sub>OD (calculation of conversion via <sup>1</sup>H-NMR spectroscopy). The calculated amounts of DAIVP and DEVV were mixed in a syringe in 0.25 mL toluene and subsequently added to the reaction solution. After 2 h, an aliquot (0.1 mL) was taken from the reaction mixture and quenched with 0.1 mL wet CD<sub>3</sub>OD (calculation of conversion via <sup>31</sup>P-NMR spectroscopy). The reaction mixture was then quenched by the addition of 0.5 mL EtOH and subsequently precipitated from pentane (50 mL). After centrifugation, the liquid phase was decanted off. The polymer was dissolved in 1,4-dioxane and lyophilized overnight. The product was obtained as a colorless solid. Each aliquot was used for SEC analysis of the A- and ABB'-polymer, respectively.

**<sup>1</sup>H-NMR** (400 MHz, MeOD, 300 K):  $\delta$  (ppm) = 8.47-7.98 (m, H<sub>Ar,P2VP</sub>), 7.55-7.22 (m, H<sub>Ar,P2VP</sub>), 7.20-6.77 (m, H<sub>Ar,P2VP</sub>), 6.24-6.62 (m, H<sub>Ar,P2VP</sub>), 6.03 (br s, H<sub>Allyl</sub>), 5.40 (d, <sup>3</sup>J = 17.2 Hz, H<sub>Allyl</sub>), 5.31-5.20 (m, H<sub>Allyl</sub>), 4.62 (br s, H<sub>CH2,PDAIVP</sub>), 4.18 (br s, H<sub>CH2,PDEVV</sub>), 2.97-1.30 (m, H<sub>Vinylphosphonate backbone</sub>), 2.00-1.50 (m, H<sub>P2VP,backbone</sub>), 1.39 (br s, H<sub>CH3,PDEVV</sub>).

**<sup>31</sup>P-NMR** (162 MHz, MeOD, 300 K):  $\delta$  (ppm) = 33.0 (br s).

The obtained intensities of the monomers vary due to the composition of the respective polymer.

## Monomer reactivity ratios of DEVP and DAIVP

The Fineman-Ross equations (*Equation (1)* and *Equation (2)*) were used to calculate the reactivity ratios of a DAIVP or DEVP-polymer chain ends towards a reaction with an DAIVP or DEVP monomer,

$$\frac{F}{f}(f - 1) = r_1 \frac{F^2}{f} - r_2 \quad (1)$$

$$\frac{f - 1}{F} = -r_2 \frac{f}{F^2} + r_1 \quad (2)$$

in which  $F$  is the monomer ratio in feed ( $F = M_1/M_2$ ; DAIVP ( $M_1$ ) and DEVP ( $M_2$ )) and  $f$  is the monomer ratio in the polymer ( $f = m_1/m_2$ ; DAIVP ( $m_1$ ) and DEVP ( $m_2$ )). Furthermore,  $r_1$  and  $r_2$  are the reactivity ratios of DAIVP and DEVP, respectively. The monomer reactivity ratios are given by  $r_1 = k_{11}/k_{12}$  and  $r_2 = k_{22}/k_{21}$ . The reactivity ratios are obtained from calculating the slopes by plotting  $(F_2/f)$  against  $(F/f)(f - 1)$  and  $(f/F_2)$  against  $(f - 1)/F$  for the determination of  $r_1$  and  $r_1$ , respectively (Figure S6).<sup>11</sup>

## Post-polymerization Functionalization of block copolymers with cysteamine hydrochloride

The respective block copolymer (100 mg, 1.0 eq. allyl-groups) was dissolved in 6.0 mL of a 1:1 mixture of MeOH and THF and the calculated amount of cysteamine hydrochloride (5.0 eq. per allyl group) and catalytic amounts of AIBN (tip of a spatula) were added and stirred at room temperature until a clear solution was observed. After degassing the reaction mixture by the repeated evacuation of the reaction volume and filling with argon (20 iterations), the reaction was started at 60 °C. After 24 h, complete conversion of the allyl groups was observed by <sup>1</sup>H NMR-spectroscopy and all volatiles were removed in vacuo. The residue was dissolved in deionized water and purified by dialysis against water (MWCO 6-8 kDa). Freeze-drying from water yielded the colorless solid.

**<sup>1</sup>H-NMR** (400 MHz, MeOD, 300 K):  $\delta$  (ppm) = 8.47-7.98 (m, 1 H, H<sub>Ar,P2VP</sub>), 7.55-7.22 (m, H<sub>Ar,P2VP</sub>), 7.20-6.77 (m, H<sub>Ar,P2VP</sub>), 6.24-6.62 (m, H<sub>Ar,P2VP</sub>), 4.21 (br s, OCH<sub>2</sub>), 3.18 (br s, CH<sub>2</sub>), 2.91 (br s, CH<sub>2</sub>), 2.78 (br s, CH<sub>2</sub>), 2.07 (br s, CH<sub>2</sub>), 2.97-1.30 (m, H<sub>Vinylphosphonate backbone</sub>), 2.00-1.50 (m, H<sub>P2VP,backbone</sub>), 1.41 (br s, CH<sub>3</sub>).

The obtained intensities of the monomers vary due to the composition of the respective polymer.

## 2) NMR Spectra of Polymers

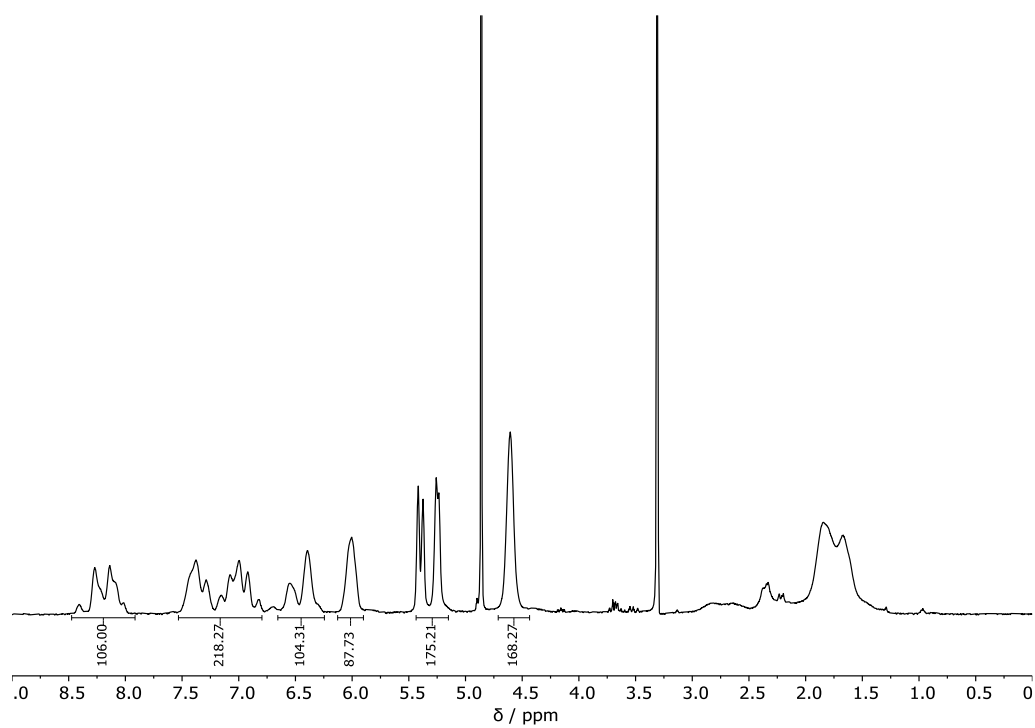


Figure S1:  $^1\text{H}$  NMR spectrum of unmodified AB-1 (MeOD- $d_4$ , 400 MHz).

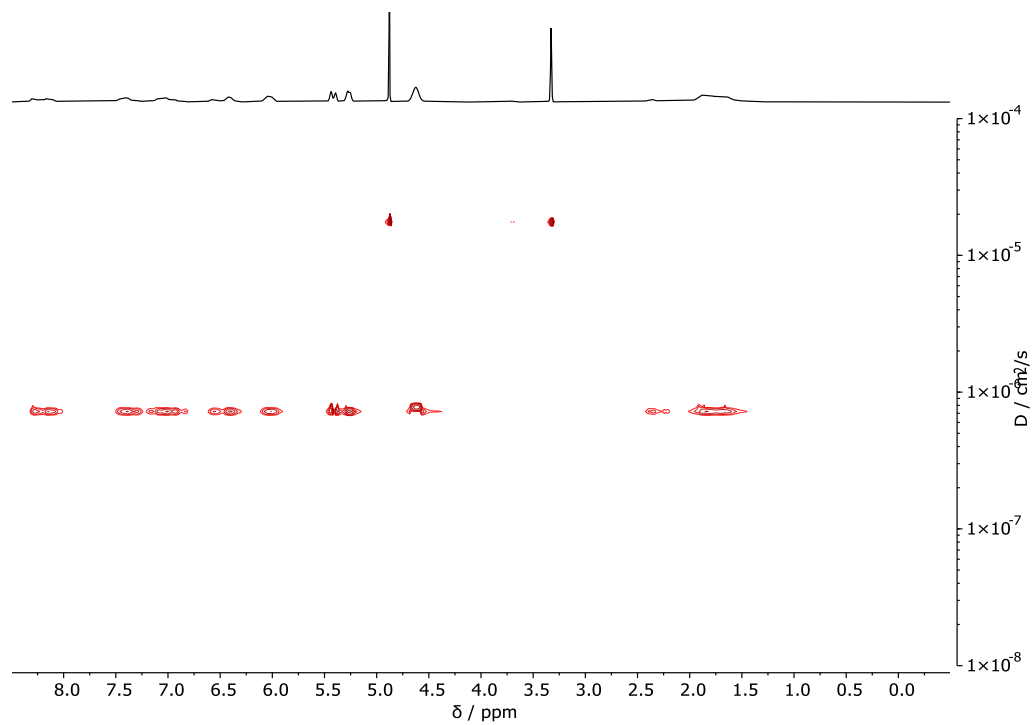


Figure S2:  $^1\text{H}$  DOSY NMR spectrum of unmodified AB-1 (MeOD- $d_4$ , 400 MHz).

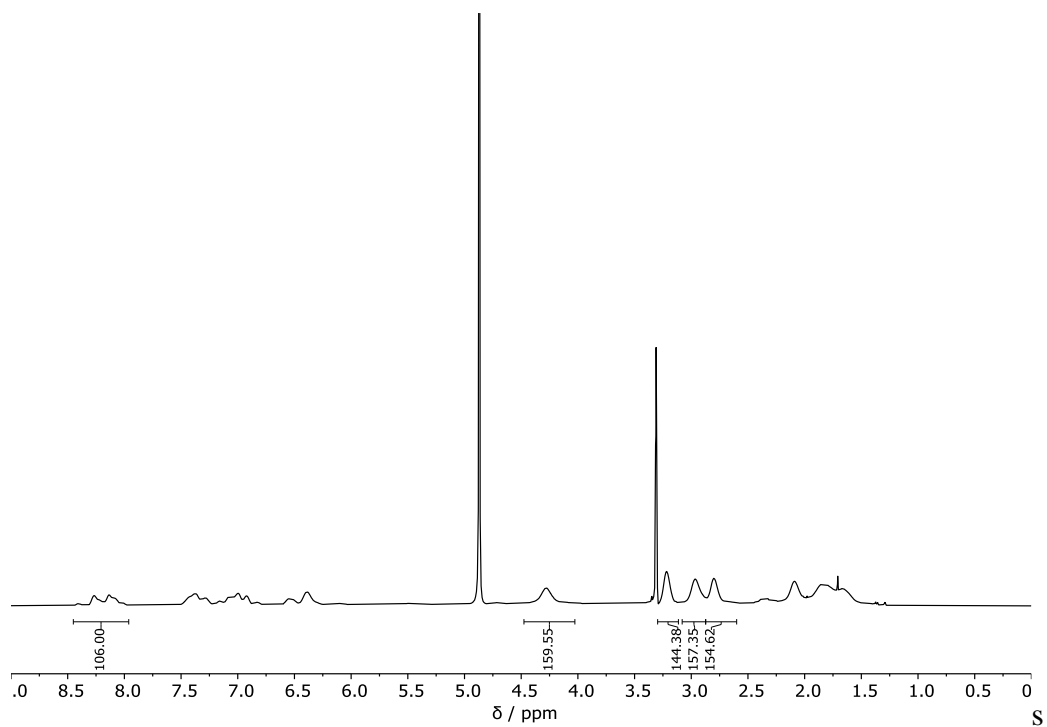


Figure S3:  $^1\text{H}$  NMR spectrum of cysteamine-modified AB-1 (MeOD- $d_4$ , 400 MHz).

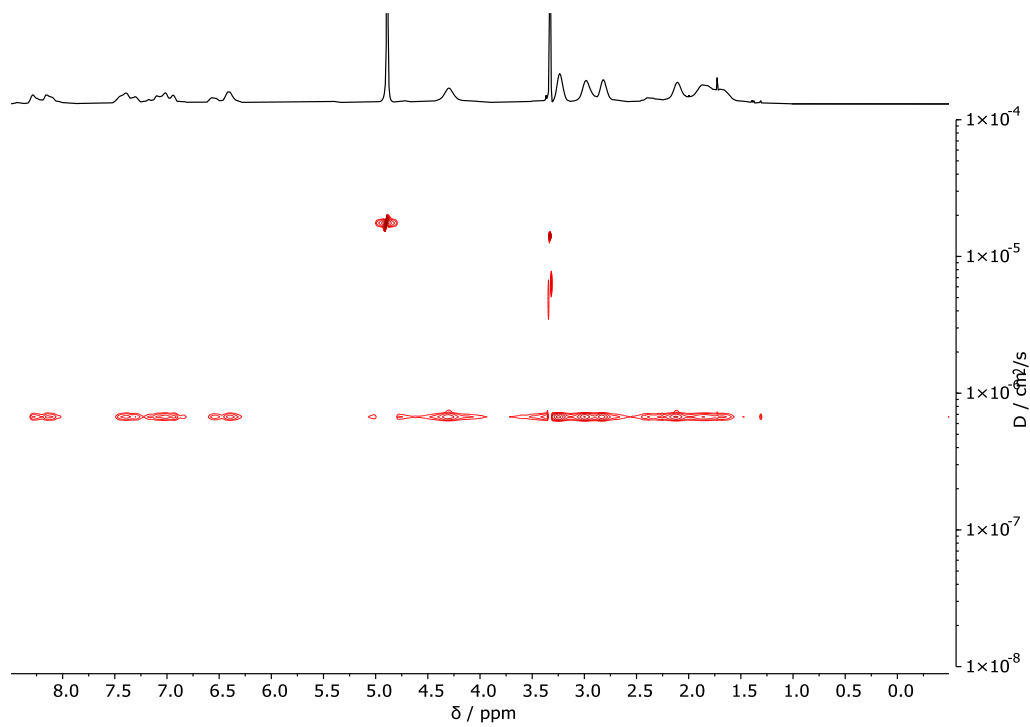


Figure S4:  $^1\text{H}$  DOSY NMR spectrum of cysteamine-modified AB-1 (MeOD- $d_4$ , 400 MHz).

### 3) SEC Trace

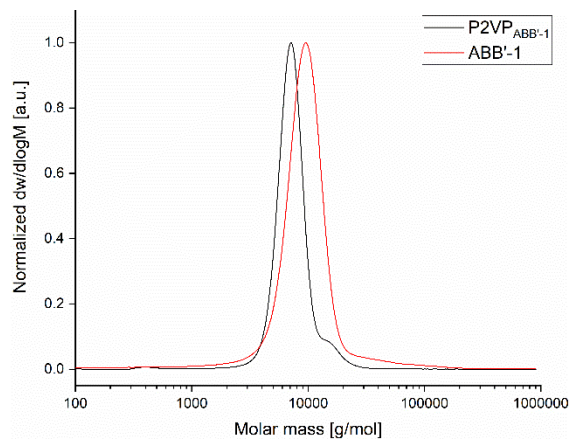


Figure S5: Exemplary SEC traces of P2VP<sub>ABB'-1</sub> (grey) and unmodified ABB'-1 (red) measured via SEC in DMF.

### 4) Fineman-Ross plots and data

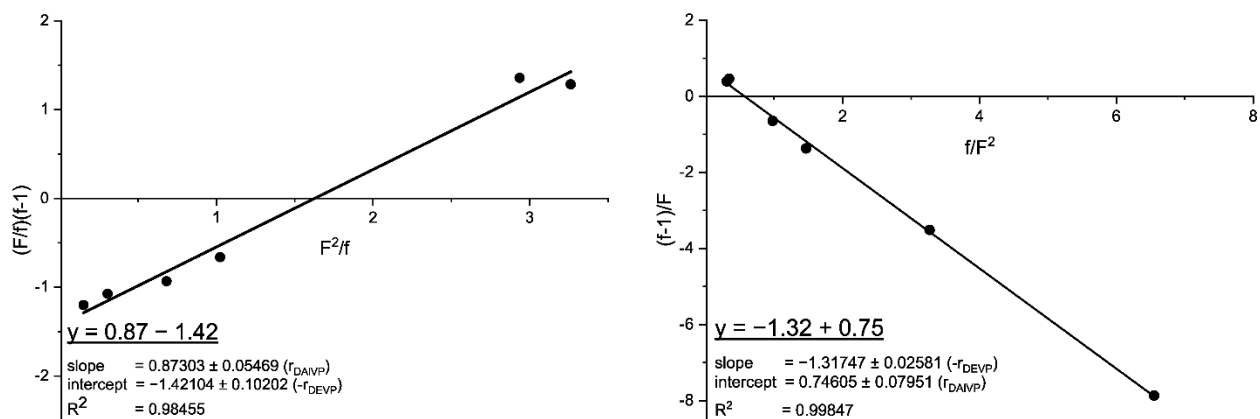


Figure S6: Fineman-Ross plots of statistical copolymerization of DEVp and DAIVP.<sup>12</sup>

## 5) Critical micelle concentration

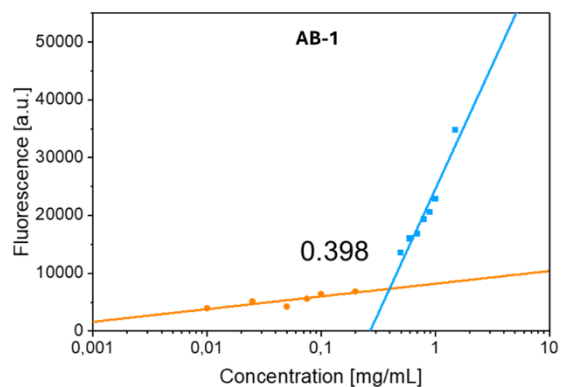


Figure S7: CMC determination of AB-1 plot using Nile red.

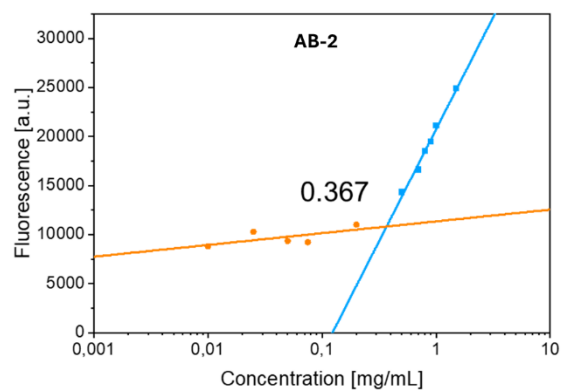


Figure S8: CMC determination of AB-2 plot using Nile red.

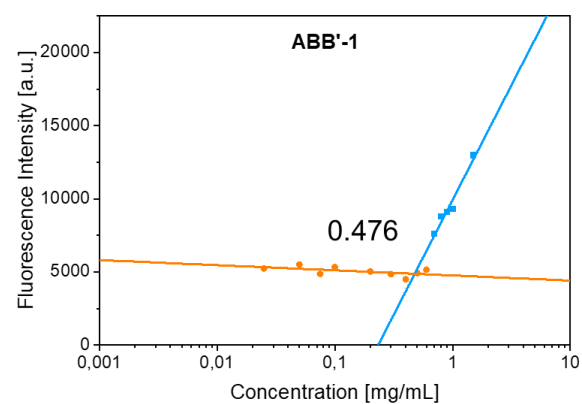


Figure S9: CMC determination of ABB'-1 plot using Nile red.

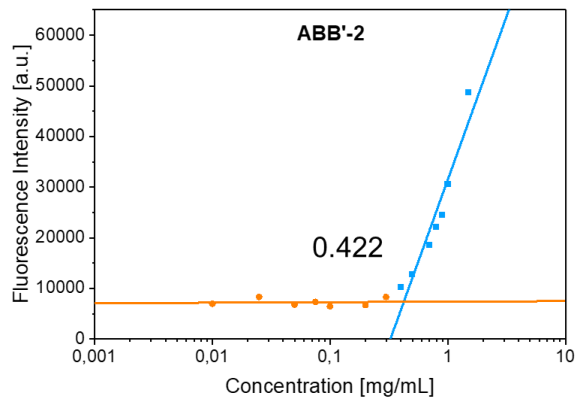


Figure S10: CMC determination of ABB'-2 plot using Nile red.

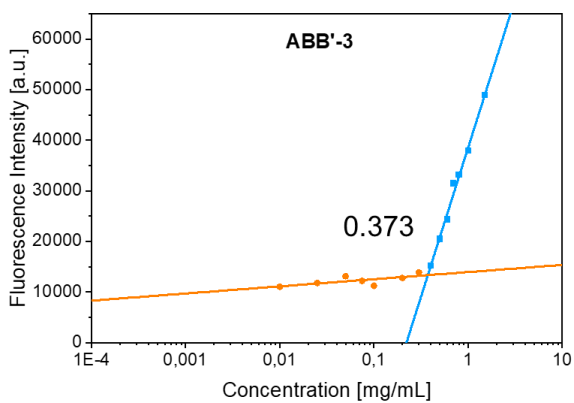


Figure S11: CMC determination of ABB'-3 plot using Nile red.

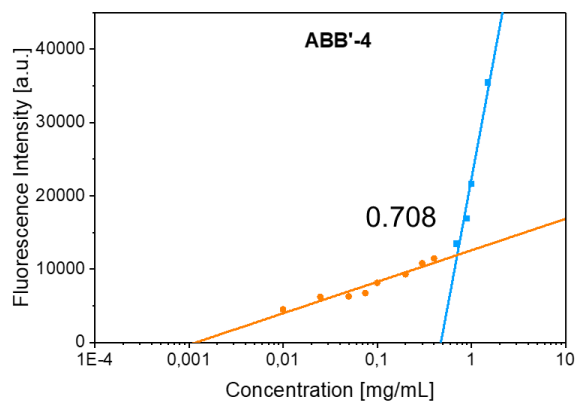


Figure S12: CMC determination of ABB'-4 plot using Nile red.

## 6) Crystal violet assay

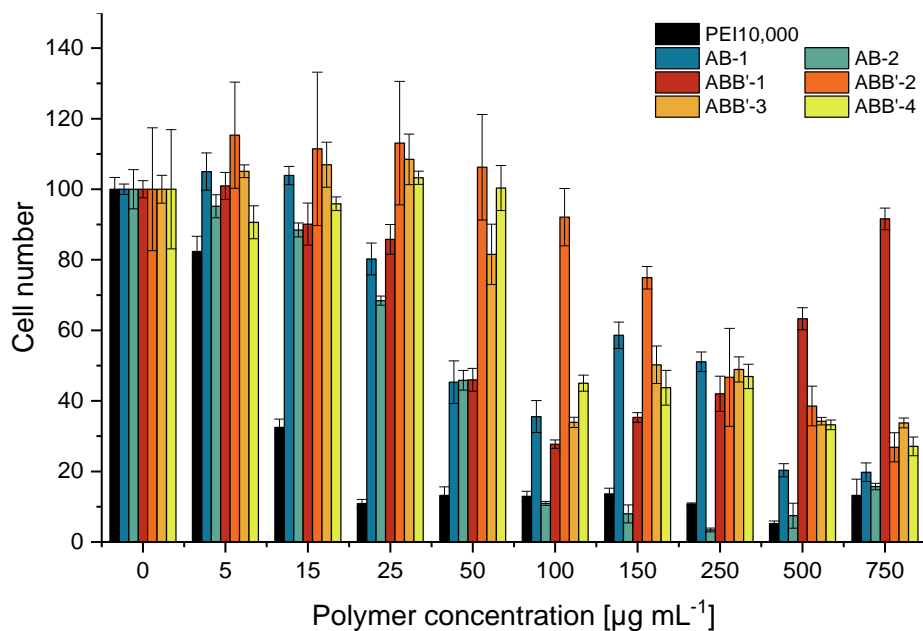


Figure S13: Crystal violet assay of AB and ABB' polymers and PEI (10 kDa).

## 7) Additional microscopic data for crystal violet assay

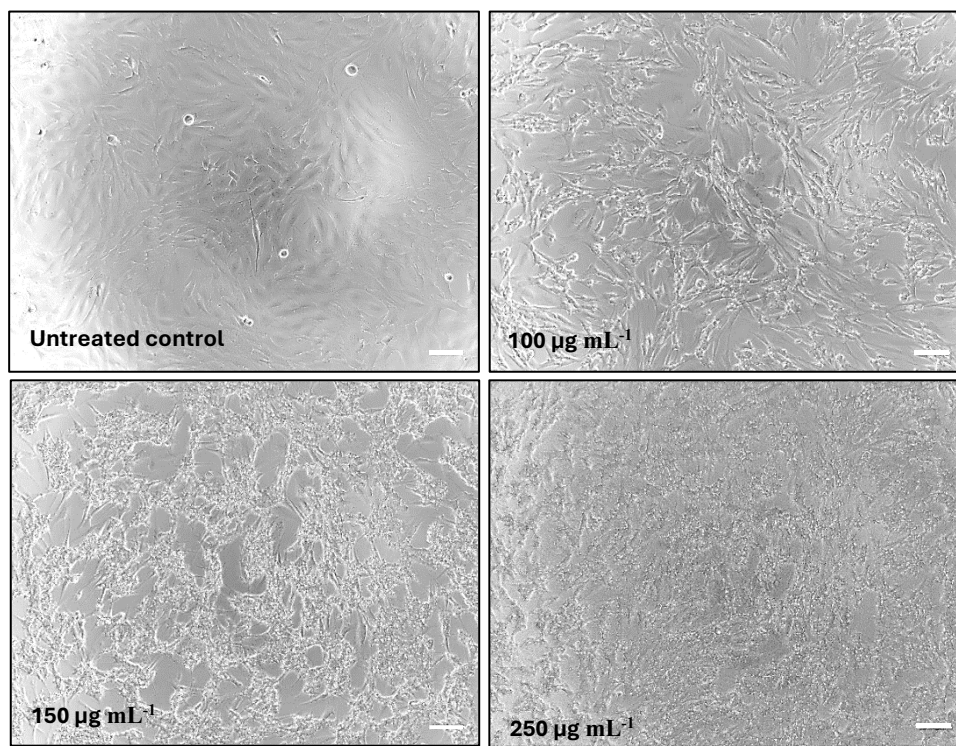


Figure S14: Representative microscopic images of MIO-M1 cell line 24 hours after being treated with AB-1. Scale bar: 100  $\mu\text{m}$ .

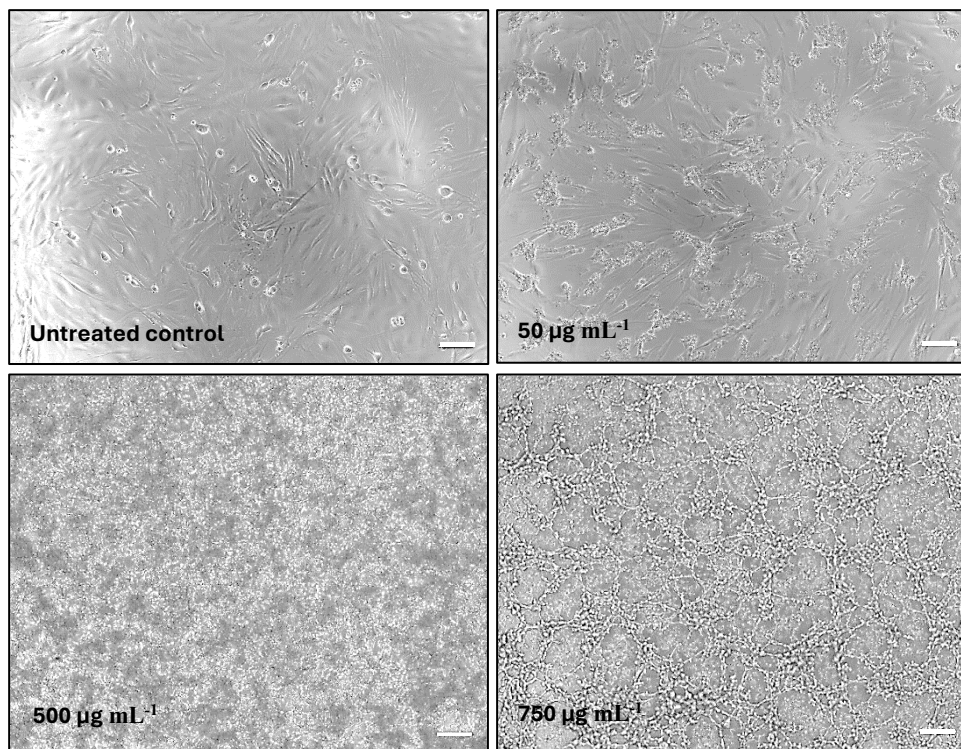


Figure S15: Representative microscopic images of MIO-M1 cell line 24 hours after being treated with AB-2. Scale bar: 100  $\mu\text{m}$ .

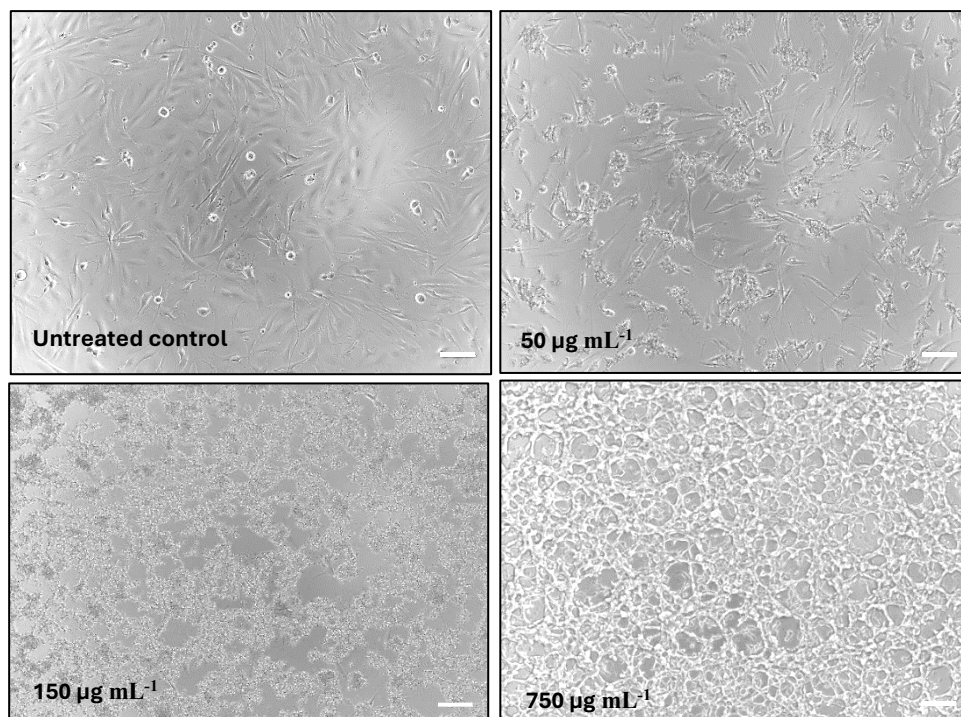


Figure S16: Representative microscopic images of MIO-M1 cell line 24 hours after being treated with ABB<sup>3</sup>-1. Scale bar: 100  $\mu\text{m}$ .

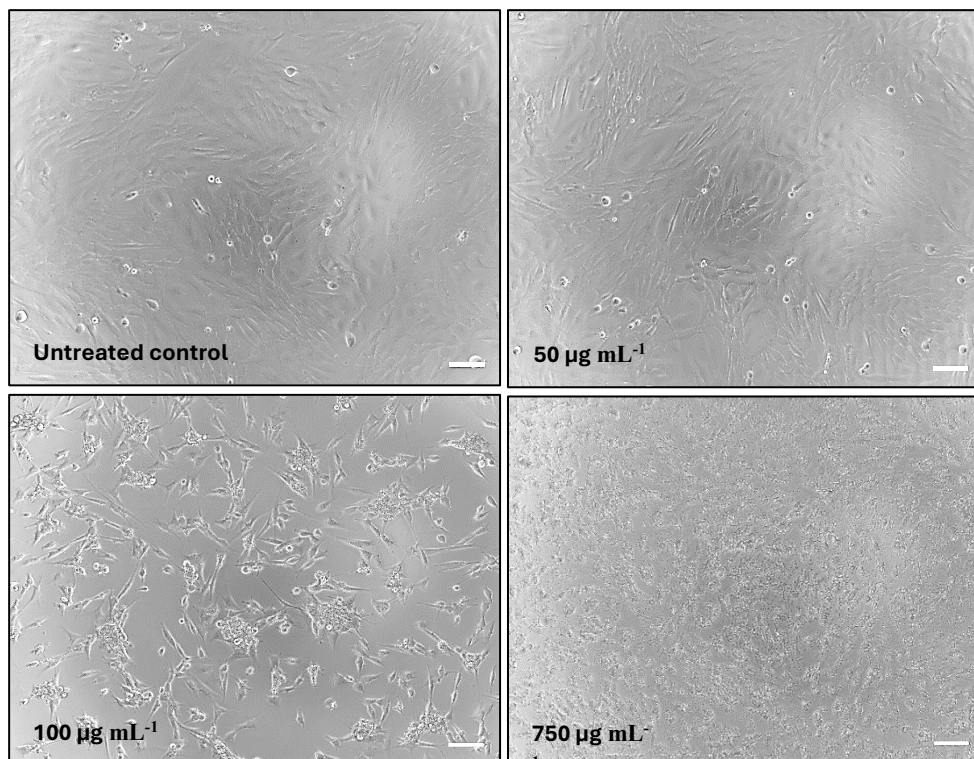


Figure S17: Representative microscopic images of MIO-M1 cell line 24 hours after being treated with ABB'-3. Scale bar: 100  $\mu\text{m}$ .

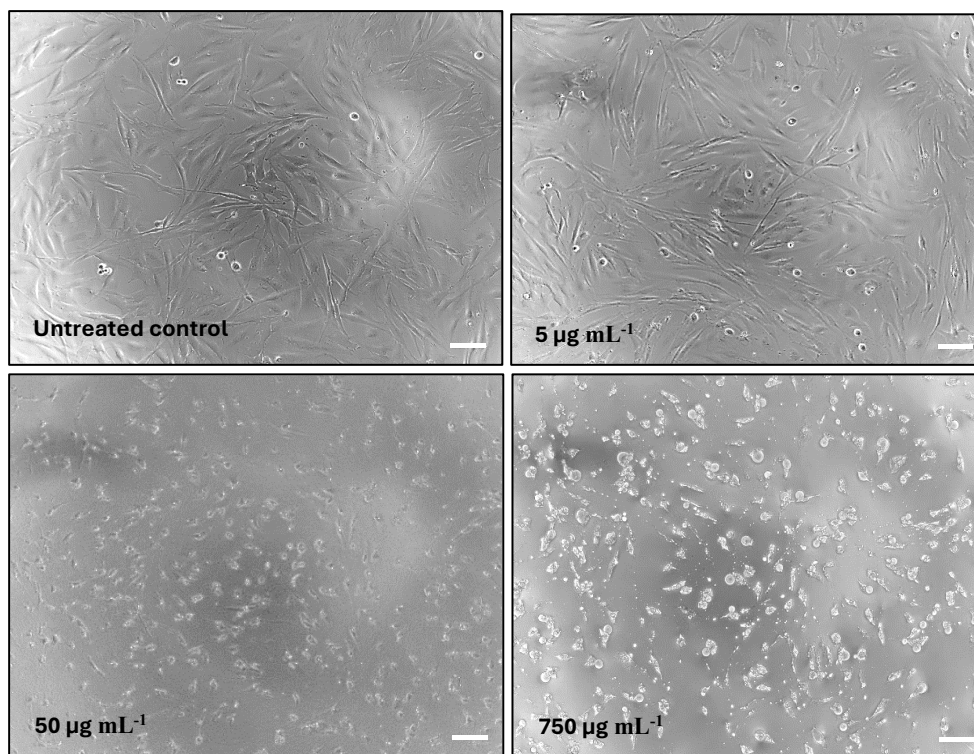


Figure S18: Representative microscopic images of MIO-M1 cell line 24 hours after being treated with PEI. Scale bar: 100  $\mu\text{m}$ .

## 8) Additional polymer characterization data

Table S1: Additional polymer characterization data.

Entry	P2VP/PDAIVP/ PDEV (A/B/B') <sup>a</sup>	$M_{n,NMR,AB(B')Allyl}$ [kg mol <sup>-1</sup> ] <sup>b</sup>	$D_{AB(B')Allyl}$ <sup>c</sup>	$M_n$ , NMR,AB(B')Cyst [kg mol <sup>-1</sup> ] <sup>d</sup>	$M_{n,A}$ [kg mol <sup>-1</sup> ] <sup>e</sup>	$M_{n,cationic}$ block,NMR [kg mol <sup>-1</sup> ] <sup>f</sup>	wt.% cationic part <sup>g</sup>	$D_{h,AB(B')Cyst}$ [nm] <sup>h</sup>	$D_{h,AB(B')Cyst}$ [nm] <sup>i</sup>
AB-1	106/44	19.4	1.14	29.4	11.1	18.3	62	292 ± 112	27 ± 6
AB-2	52/56	16.0	1.17	28.7	5.5	23.3	81	140 ± 91	20 ± 7
ABB'-1	85/71/44	29.5	1.13	45.7	8.9	29.5	65	193 ± 70	26 ± 5
ABB'-2	156/31/59	31.9	1.12	39.0	16.4	12.9	33	126 ± 97	24 ± 8
ABB'-3	75/36/77	27.3	1.17	35.5	7.9	15.0	42	201 ± 74	126 ± 49
ABB'-4	37/25/123	28.8	1.07 <sup>j</sup>	34.5	3.9	10.4	30	184 ± 74	99 ± 40

<sup>a</sup>A = P2VP, B = PDAIVP, B' = PDEV. BB' notation indicates statistical copolymerization. Copolymer composition determined via integration of P2VP aromatic signals versus phosphonate signals in <sup>1</sup>H NMR spectra. <sup>b</sup>Calculated molecular weight of the block copolymer via copolymer composition and  $M_{n,abs,A}$  of block A (absolute molecular weight determination of the P2VP block (SEC in DMF, 30 °C, with 25 mmol L<sup>-1</sup> LiBr, triple detection,  $dn/dc = 0.149$  mL g<sup>-1</sup>). <sup>c</sup>Determination of polydispersity of block copolymers via SEC in DMF. <sup>d</sup>Calculated molecular weight of cysteamine-modified polymer via <sup>1</sup>H NMR spectroscopy and  $M_{n,NMR,AB(B')Allyl}$ . <sup>e</sup>Absolute molecular weight determination of the P2VP block (SEC in DMF, 30 °C, with 25 mmol L<sup>-1</sup> LiBr, triple detection,  $dn/dc = 0.149$  mL g<sup>-1</sup>). <sup>f</sup>Calculated molecular weight of cationic block via <sup>1</sup>H NMR spectroscopy and the initial molecular weight of the PDAIVP block of the unmodified polymer. <sup>g</sup>Calculation of the wt% of the cationic part with respect to the molecular weight of the cysteamine-modified block copolymer: wt.%(cationic part) =  $M_{n,cationic,block,NMR}/M_{n,NMR,AB(B')Cyst}$ . <sup>h</sup>Determined *via* DLS. Intensity mean of main peak and standard deviation given as peak width. <sup>i</sup>Determined *via* DLS. Number mean and standard deviation given as peak width. <sup>j</sup>Determination of polydispersity of ABB'-4 *via* SEC in THF/H<sub>2</sub>O (1/1) using SEC-MALS.

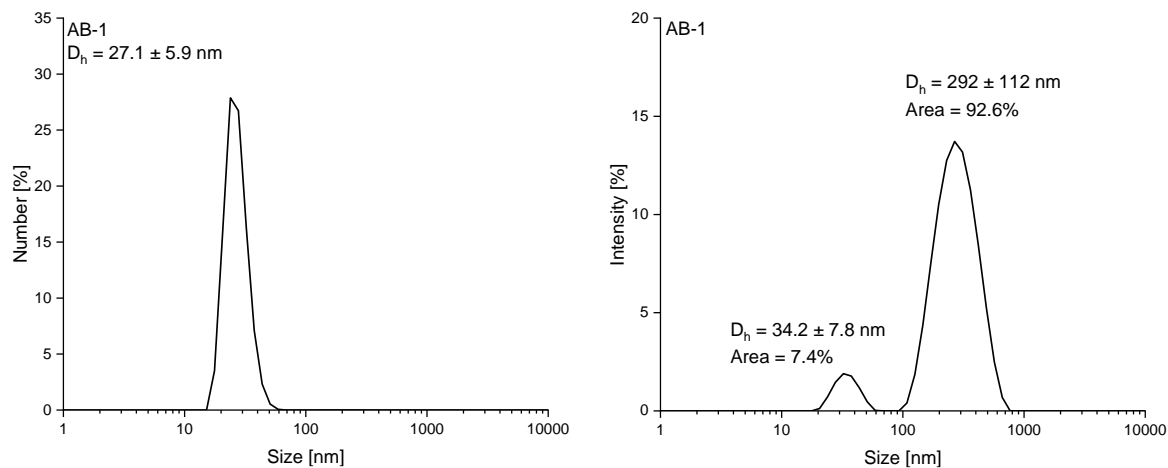


Figure S19: Size distributions reported as peak mean ± peak width by number (left) and intensity (right) of AB-1.

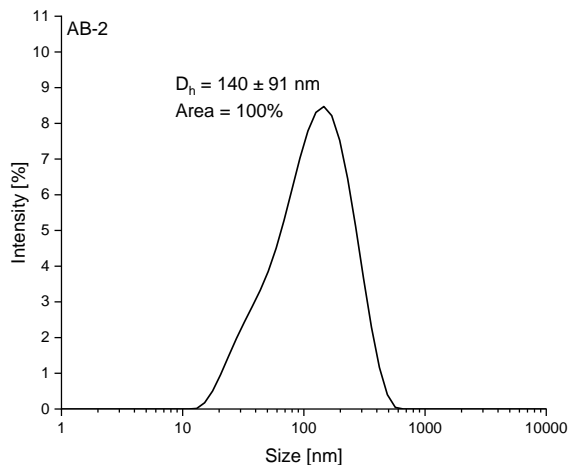
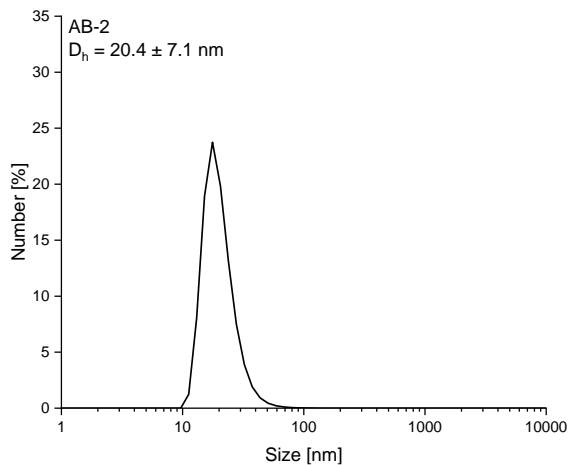


Figure S20: Size distributions as peak mean  $\pm$  peak width by number (left) and intensity (right) of AB-2.

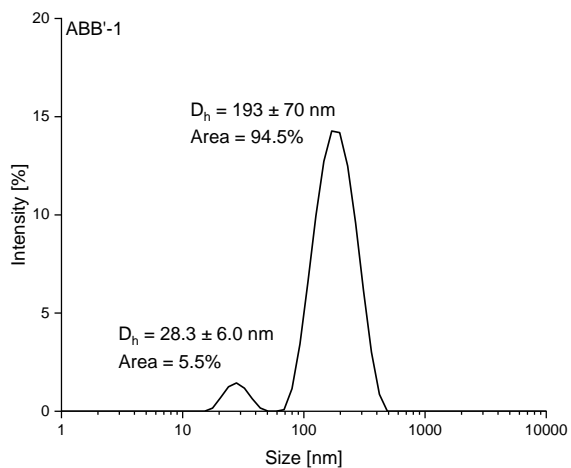
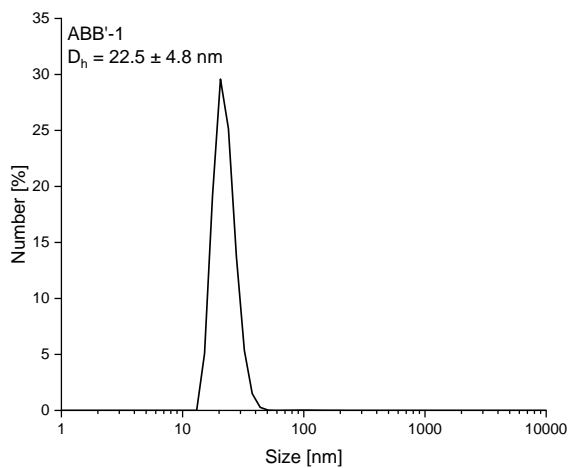


Figure S21: Size distributions as peak mean  $\pm$  peak width by number (left) and intensity (right) of ABB'-1.

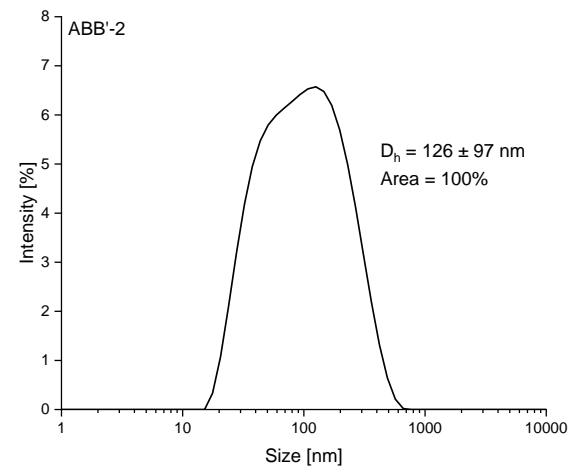
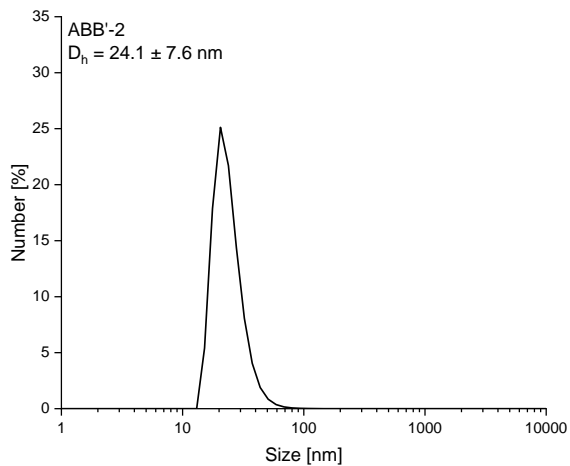


Figure S22: Size distributions as peak mean  $\pm$  peak width by number (left) and intensity (right) ABB'-2.

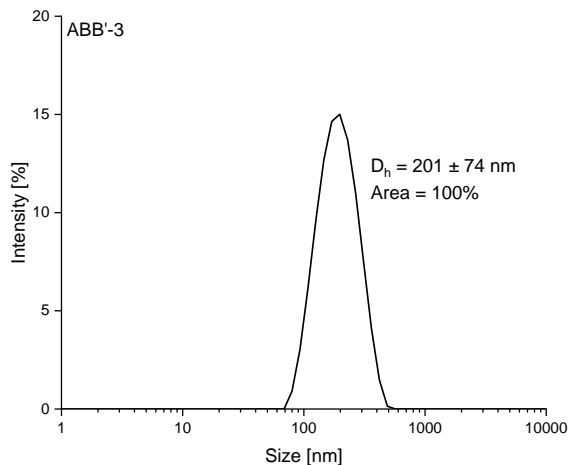
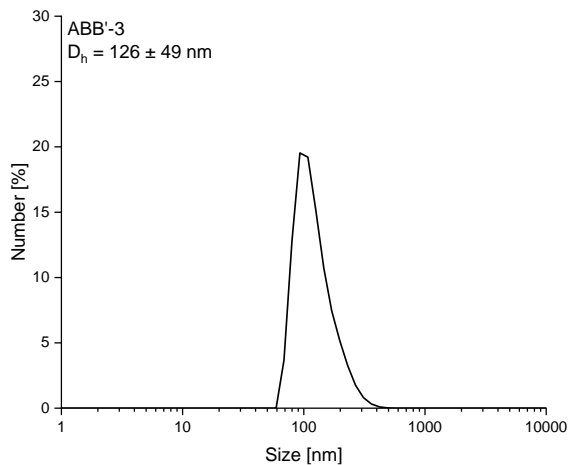


Figure S23: Size distributions as peak mean  $\pm$  peak width by number (left) and intensity (right) ABB'-3.

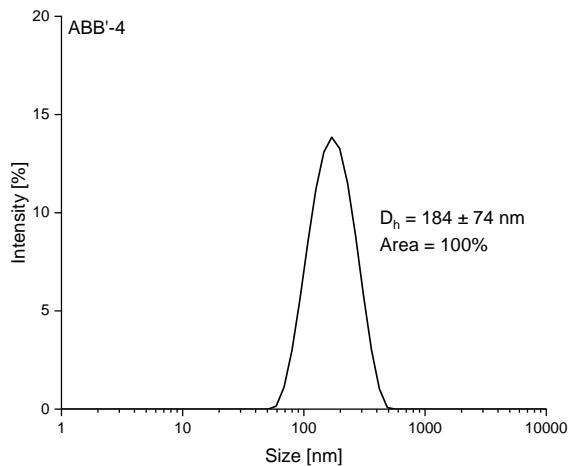
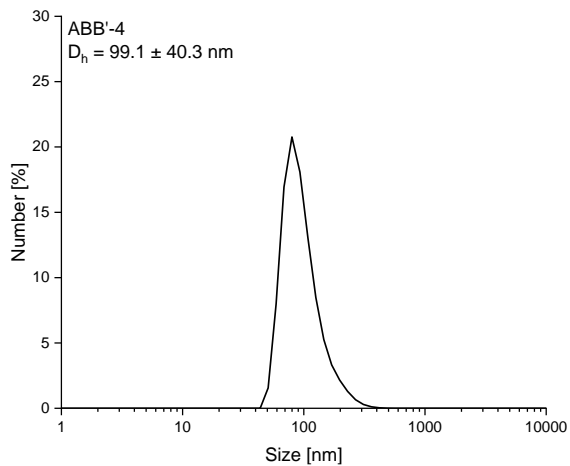


Figure S24: Size distributions as peak mean  $\pm$  peak width by number (left) and intensity (right) ABB'-4.

## 9) Additional SYBR Gold Assay evaluation

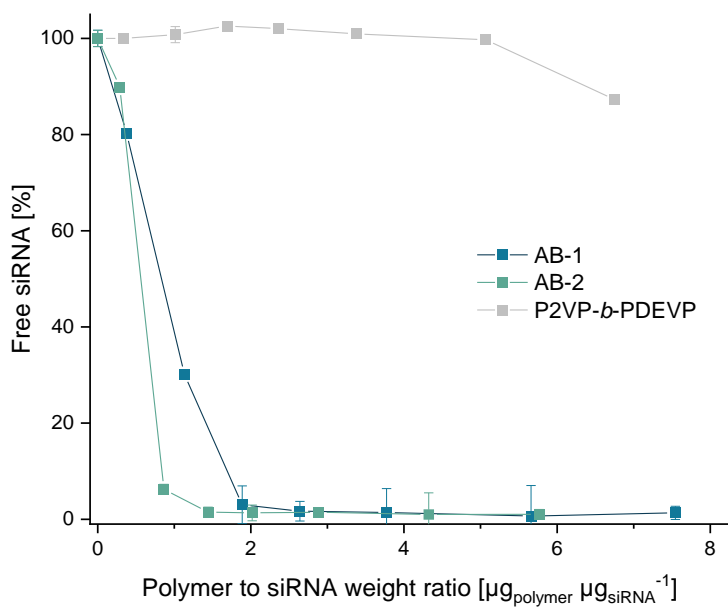


Figure S25: SYBR gold assay comparing weight ratios of cationic polymers with non-functionalized P2VP-*b*-PDEVp.

## 10) Titration Curves

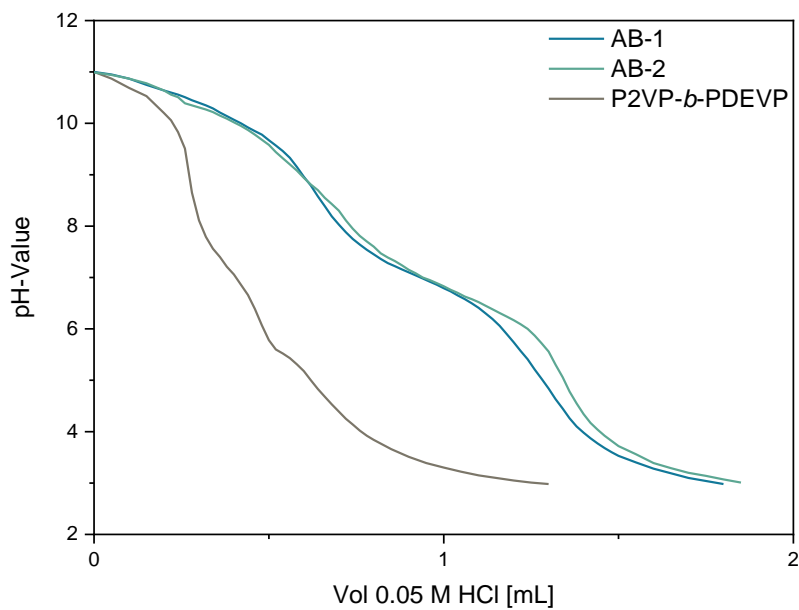


Figure S26: Titration curves of AB-type block copolymers.

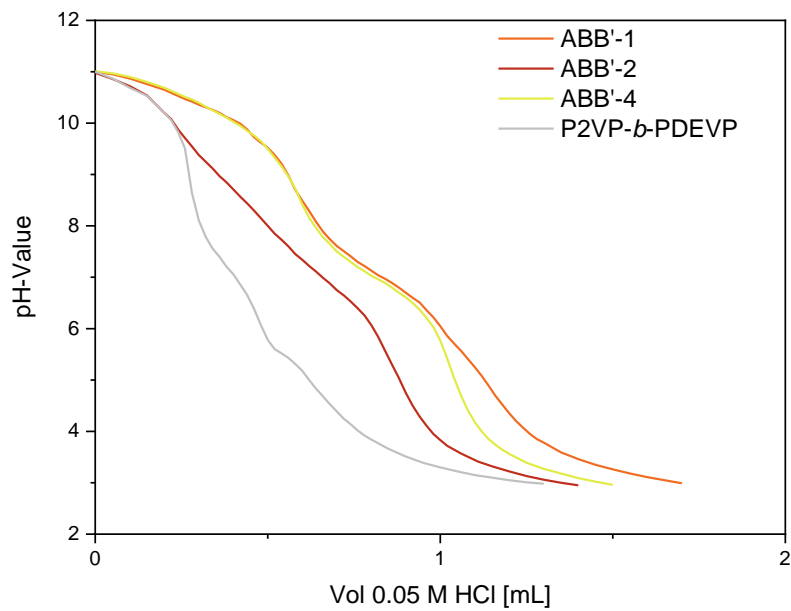


Figure S27: Titration curves of polymer ABB'-type block copolymers.

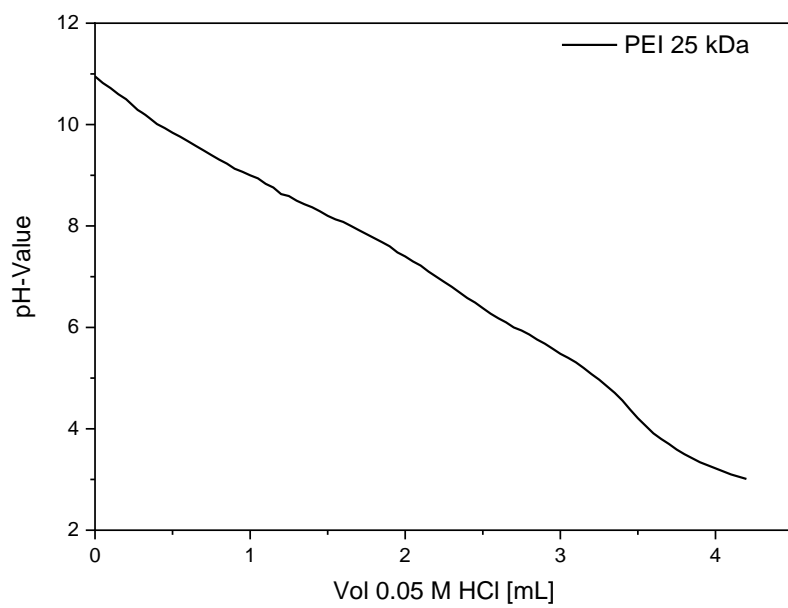


Figure S28: Titration curve of hyperbranched PEI.

## 11) Additional data for Calcein assay

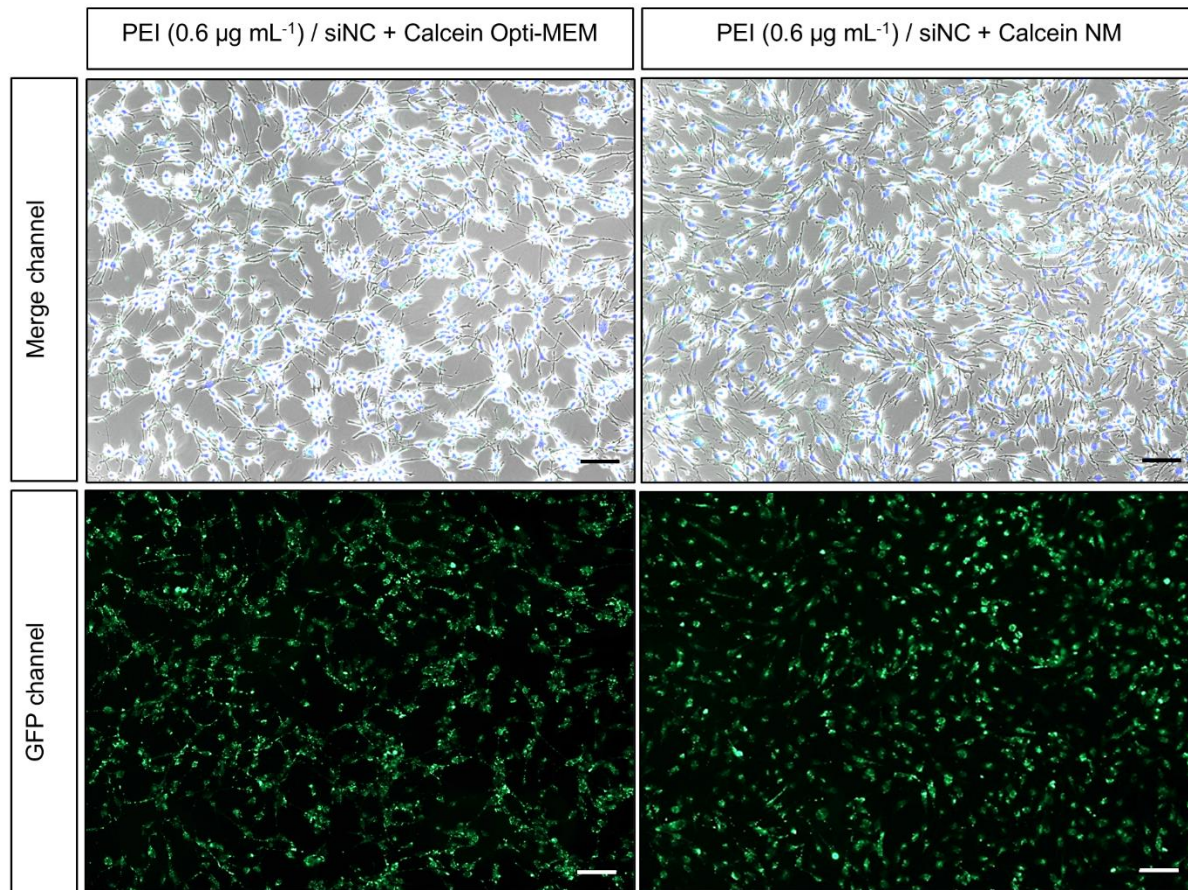


Figure S29: Representative microscopic images of MIO-M1 cell line 4 hours after being treated with PEI/siNC (N/P=2.0) and 150  $\mu\text{g mL}^{-1}$  Calcein in Opti-MEM (left), or normal medium (high glucose DMEM-F/12 containing 10% FBS; NM) (right) for 4 hours. Nuclei were stained with Hoechst dye while the Calcein signal is shown in the GFP channel. Scale bar: 100  $\mu\text{m}$ .

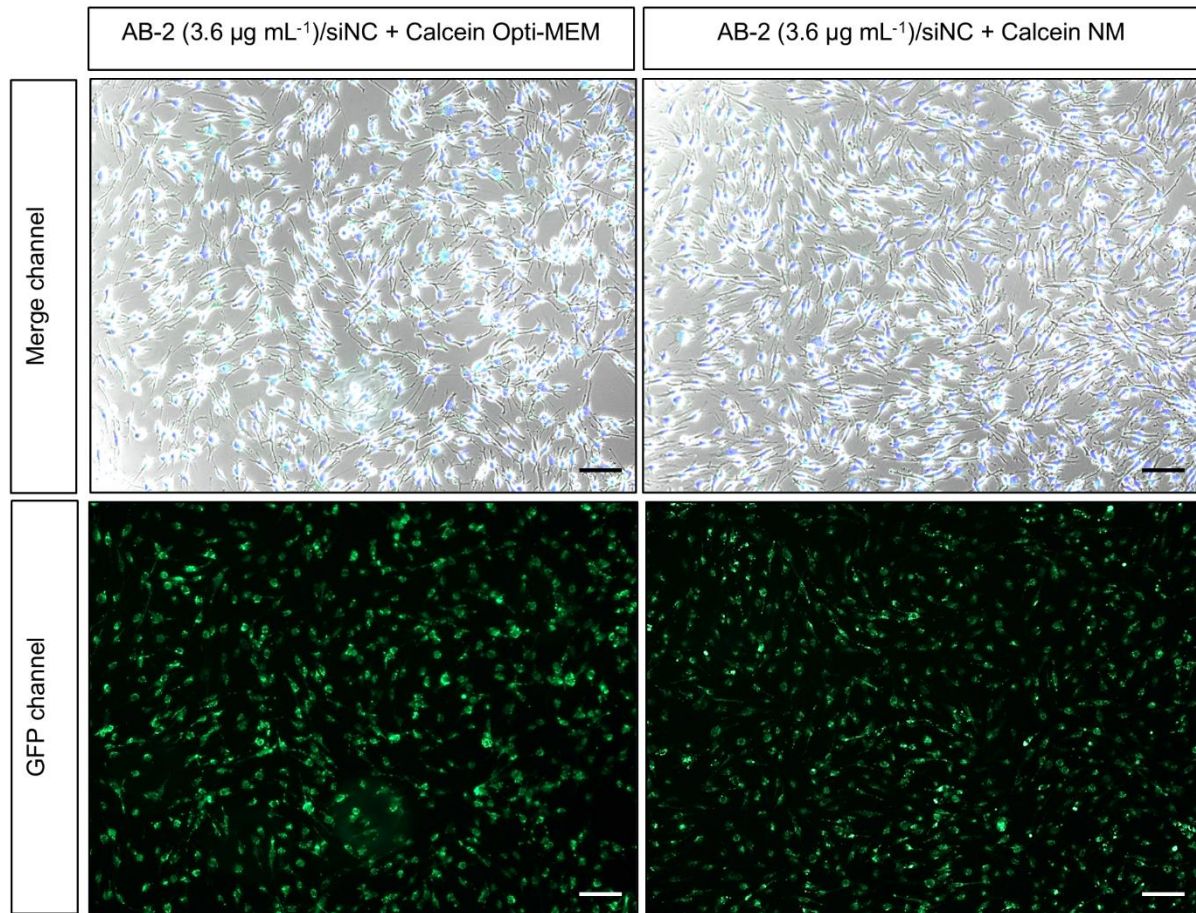


Figure S30: Representative microscopic images of MIO-M1 cell line 4 hours after being treated with AB-2/siNC (N/P=2.0) and  $150 \mu\text{g mL}^{-1}$  Calcein in Opti-MEM (left), or normal medium (high glucose DMEM-F/12 containing 10% FBS; NM) (right) for 4 hours. Nuclei were stained with Hoechst dye while the Calcein signal is shown in the GFP channel. Scale bar:  $100 \mu\text{m}$ .

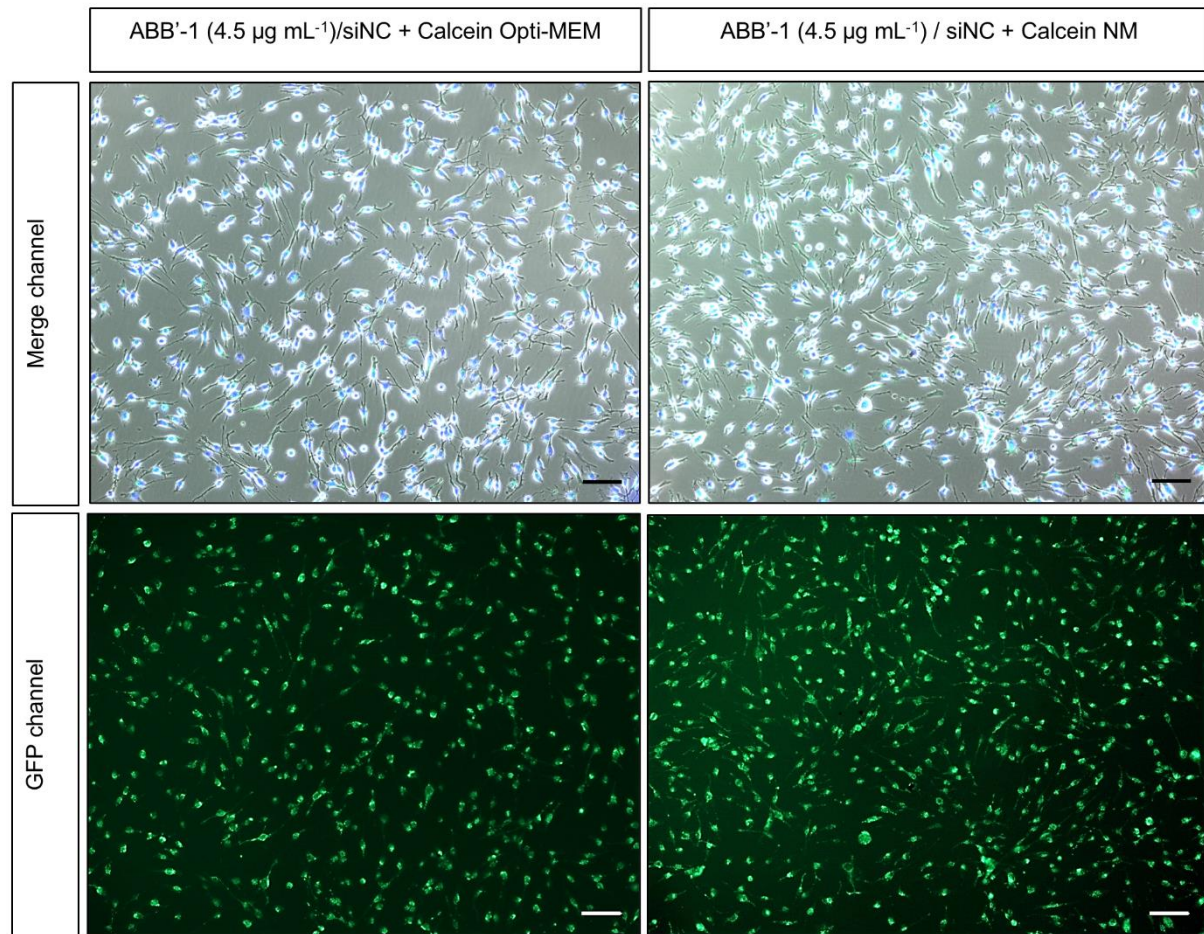


Figure S31: Representative microscopic images of MIO-M1 cell line 4 hours after being treated with ABB'-1/siNC (N/P=2.0) and 150  $\mu\text{g mL}^{-1}$  Calcein in Opti-MEM (left), or normal medium (high glucose DMEM-F/12 containing 10% FBS; NM) (right) for 4 hours. Nuclei were stained with Hoechst dye while the Calcein signal is shown in the GFP channel. Scale bar: 100  $\mu\text{m}$ .

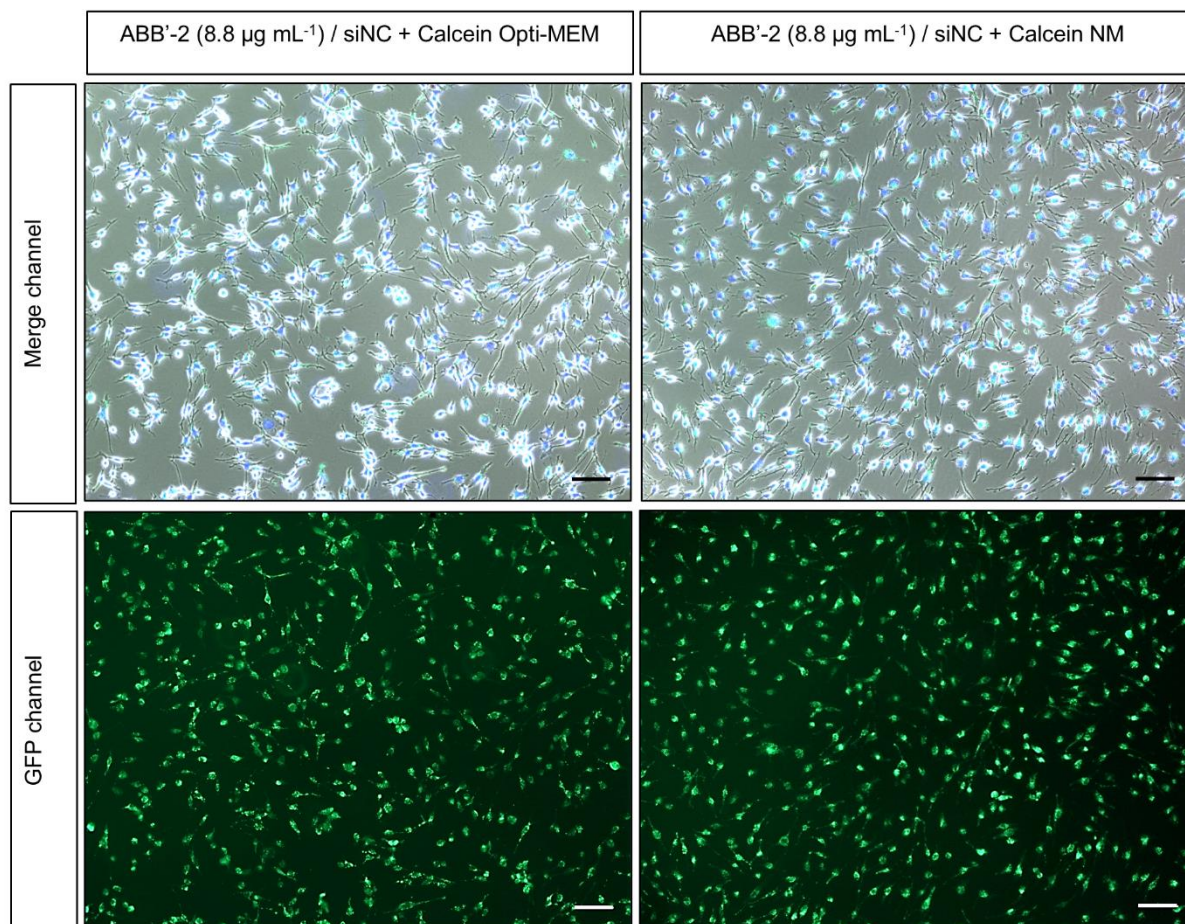


Figure S32: Representative microscopic images of MIO-M1 cell line 4 hours after being treated with ABB'-2/siNC (N/P=2.0) and 150  $\mu\text{g mL}^{-1}$  Calcein in Opti-MEM (left), or normal medium (high glucose DMEM-F/12 containing 10% FBS; NM) (right) for 4 hours. Nuclei were stained with Hoechst dye while the Calcein signal is shown in the GFP channel. Scale bar: 100  $\mu\text{m}$ .

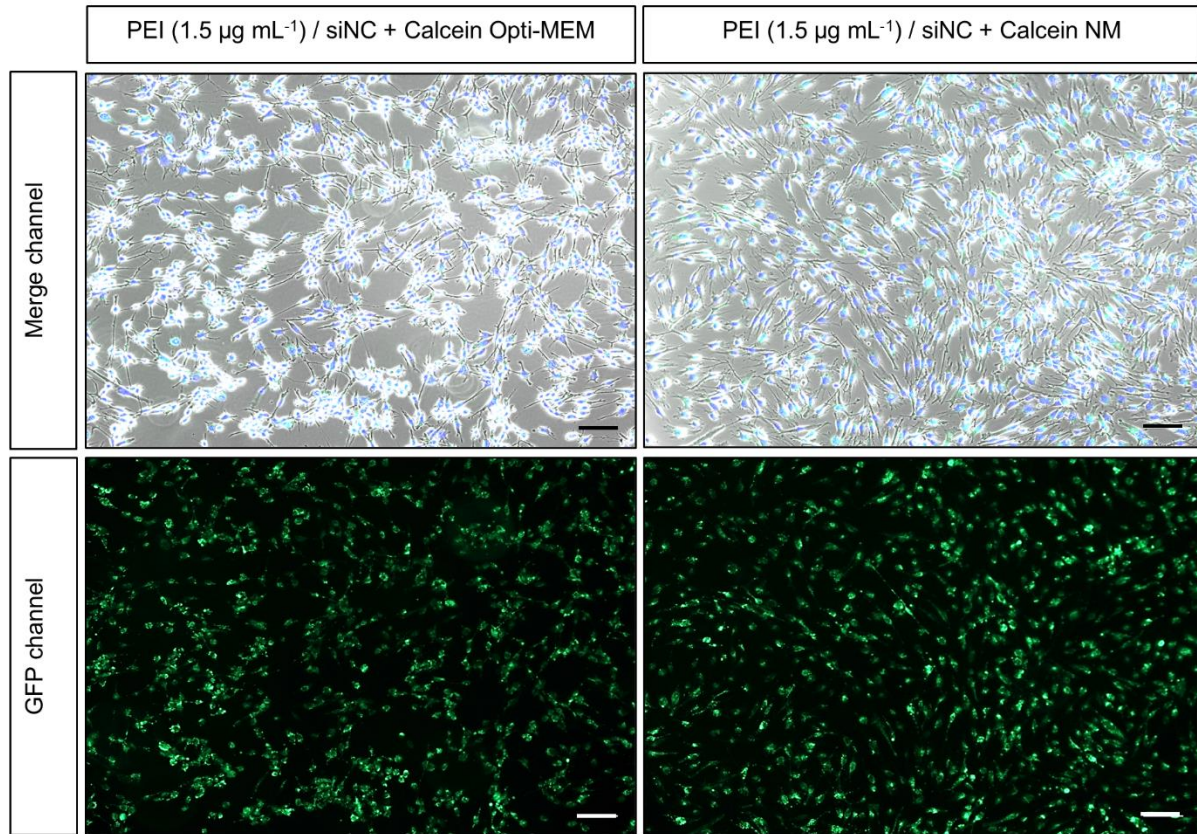


Figure S33: Representative microscopic images of MIO-M1 cell line 4 hours after being treated with PEI/siNC (N/P=5.0) and 150  $\mu\text{g mL}^{-1}$  Calcein in Opti-MEM, or normal medium (high glucose DMEM-F/12 containing 10% FBS; NM) for 4 hours. Nuclei were stained with Hoechst dye while the Calcein signal is shown in the GFP channel. Scale bar: 100  $\mu\text{m}$ .

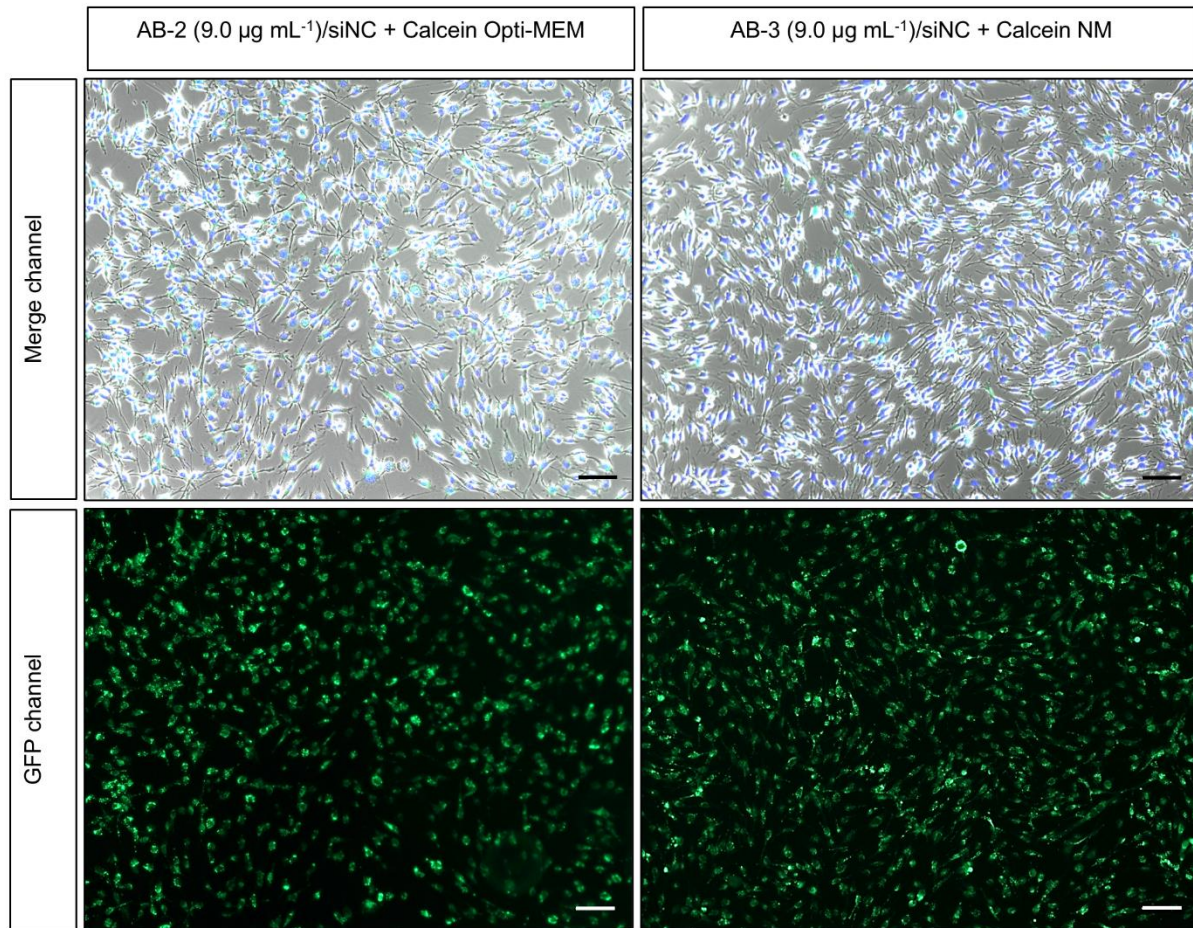


Figure S34: Representative microscopic images of MIO-M1 cell line 4 hours after being treated with AB-2/siNC (N/P=5.0) and  $150 \mu\text{g mL}^{-1}$  Calcein in Opti-MEM, or normal medium (high glucose DMEM-F/12 containing 10% FBS; NM) for 4 hours. Nuclei were stained with Hoechst dye while the Calcein signal is shown in the GFP channel. Scale bar: 100  $\mu\text{m}$ .

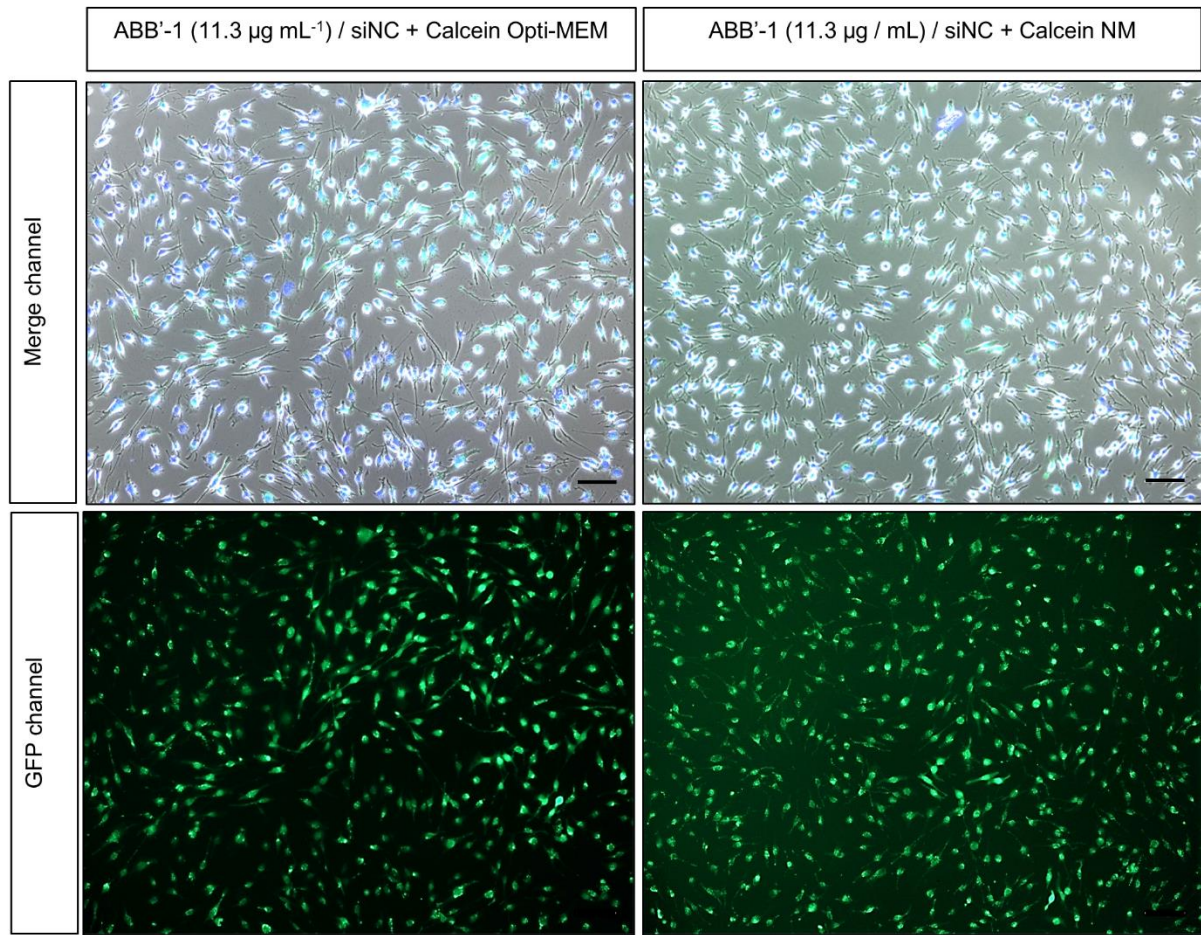


Figure S35: Representative microscopic images of MIO-M1 cell line 4 hours after being treated with ABB'-1/siNC (N/P=5.0) and 150  $\mu\text{g mL}^{-1}$  Calcein in Opti-MEM, or normal medium (high glucose DMEM-F/12 containing 10% FBS; NM) for 4 hours. Nuclei were stained with Hoechst dye while the Calcein signal is shown in the GFP channel. Scale bar: 100  $\mu\text{m}$ .

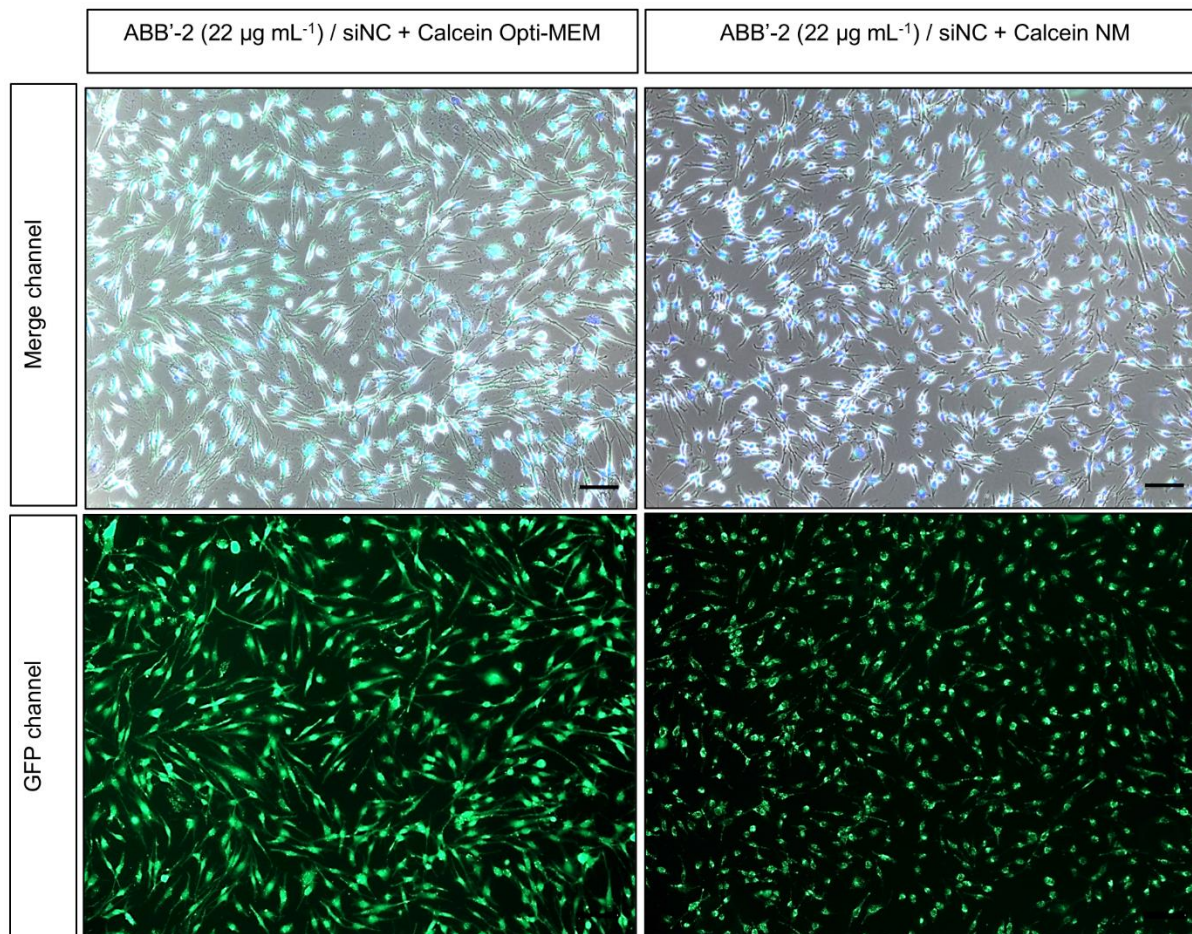


Figure S36: Representative microscopic images of MIO-M1 cell line 4 hours after being treated with ABB'-2/siNC (N/P=5.0) and 150 µg mL<sup>-1</sup> Calcein in Opti-MEM, or normal medium (high glucose DMEM-F/12 containing 10% FBS; NM) for 4 hours. Nuclei were stained with Hoechst dye while the Calcein signal is shown in the GFP channel. Scale bar: 100 µm.

## 12) DLS Data for Polyplexes

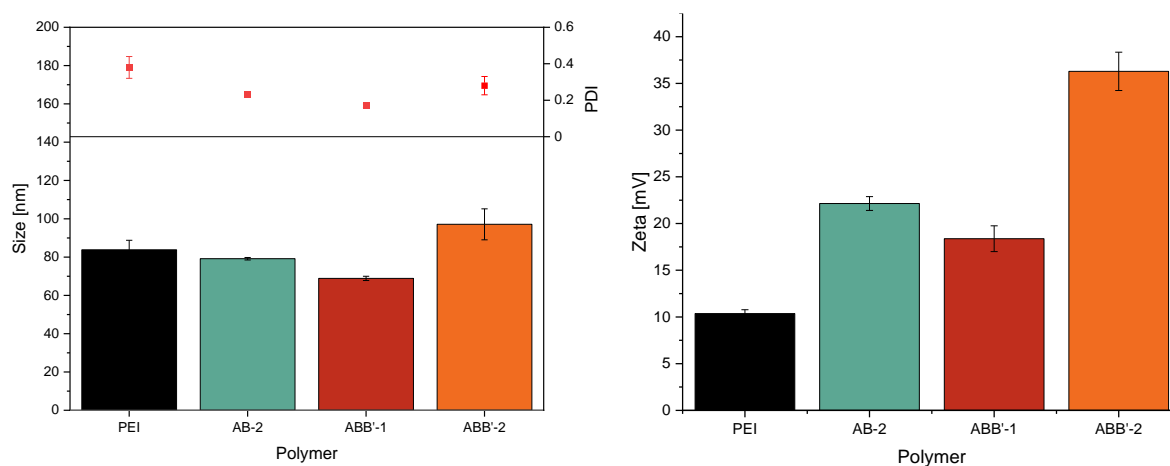


Figure S37: Size distributions (z-average, PDI) and zeta potential of polymer/siNC complexes at N/P = 5.0.

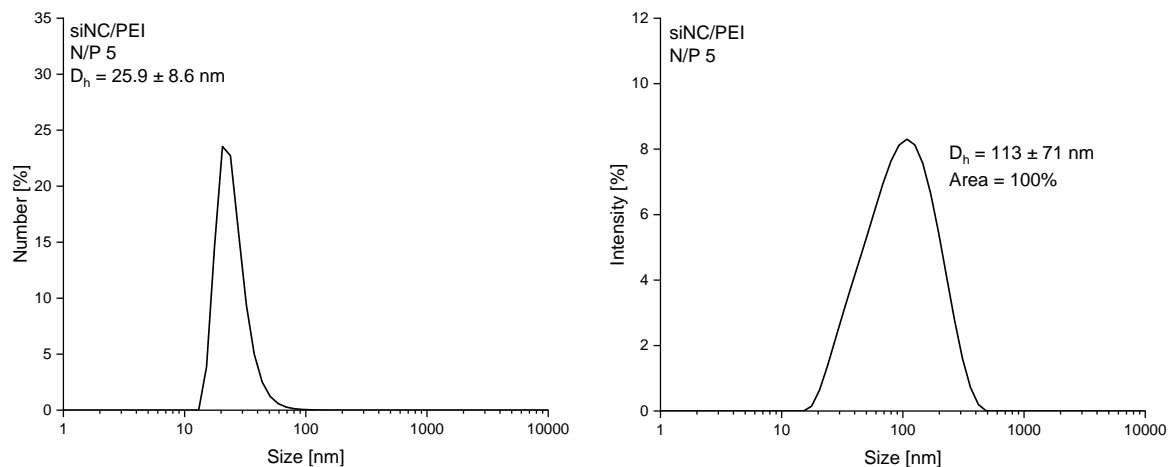


Figure S38: Size distributions as peak mean  $\pm$  peak width by number (left) and intensity (right) of siNC/PEI polyplexes at N/P = 5.0.

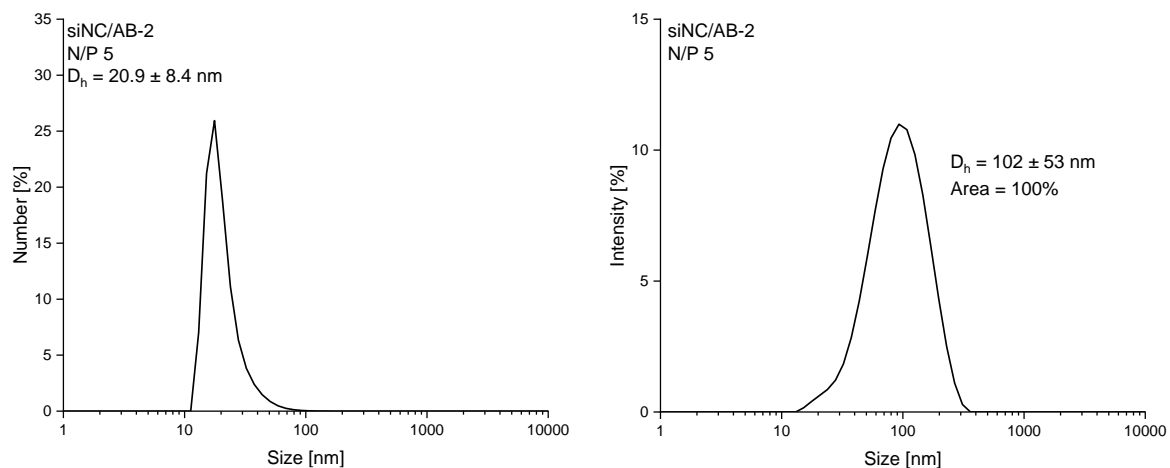


Figure S39: Size distributions as peak mean  $\pm$  peak width by number (left) and intensity (right) of siNC/AB-2 polyplexes at N/P = 5.0.

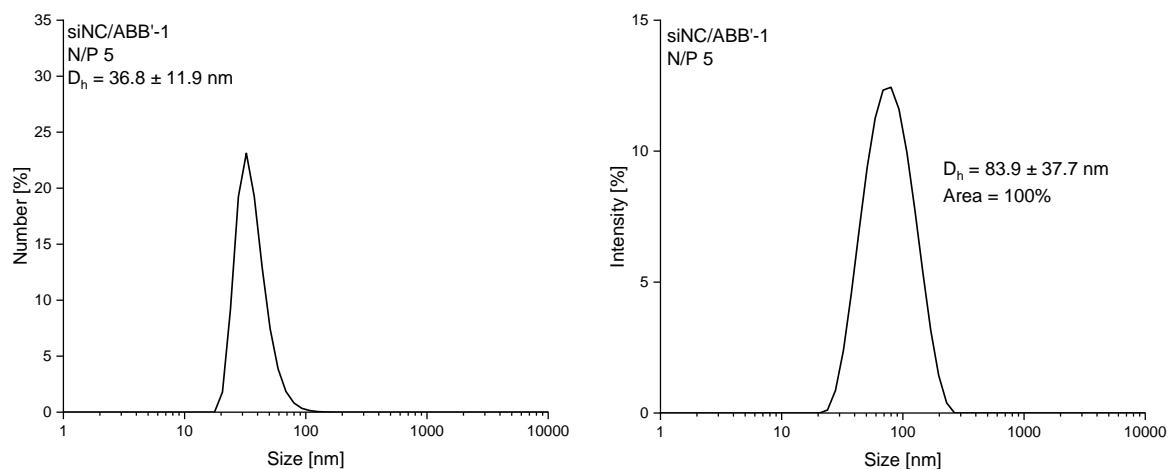


Figure S40: Size distributions as peak mean  $\pm$  peak width by number (left) and intensity (right) of siNC/ABB'-1 polyplexes at N/P = 5.0.

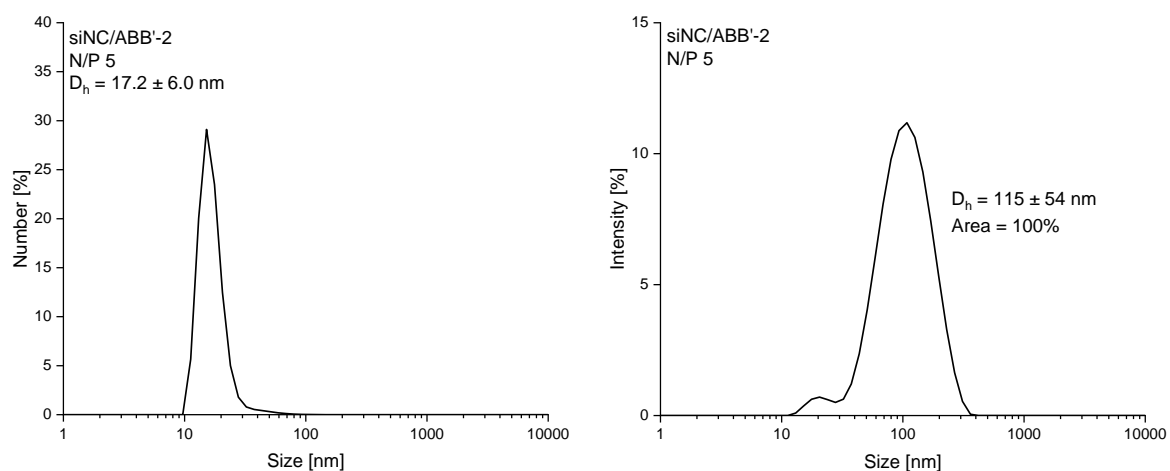


Figure S41: Size distributions as peak mean  $\pm$  peak width by number (left) and intensity (right) of siNC/ABB'-2 polyplexes at N/P = 5.0.

Table S2: Size distributions for siNC/Polymer polyplexes at N/P = 5.0 determined *via* DLS.

Polyplex at N/P = 5.0	Z-Average [nm] <sup>a</sup>	PDI <sup>a</sup>	Intensity peak mean[nm] <sup>b</sup>	Number peak mean [nm] <sup>c</sup>
PEI/siNC	$83.8 \pm 5.0$	$0.38 \pm 0.06$	$113 \pm 71$	$26 \pm 7$
AB-2/siNC	$79.1 \pm 0.6$	$0.23 \pm 0.01$	$102 \pm 53$	$21 \pm 8$
ABB'-1/siNC	$68.9 \pm 1.1$	$0.17 \pm 0.01$	$84 \pm 38$	$37 \pm 12$
ABB'-2/siNC	$97.1 \pm 8.1$	$0.28 \pm 0.05$	$115 \pm 54$	$17 \pm 6$

<sup>a</sup> Determined *via* DLS. Intensity mean of main peak and standard deviation given as peak width. <sup>b</sup> Determined *via* DLS. peak mean and standard deviation given as peak width from size distribution by intensity. <sup>c</sup> Determined *via* DLS. peak mean and standard deviation given as peak width from size distribution by intensity.

### 13) Additional data for western blot analysis

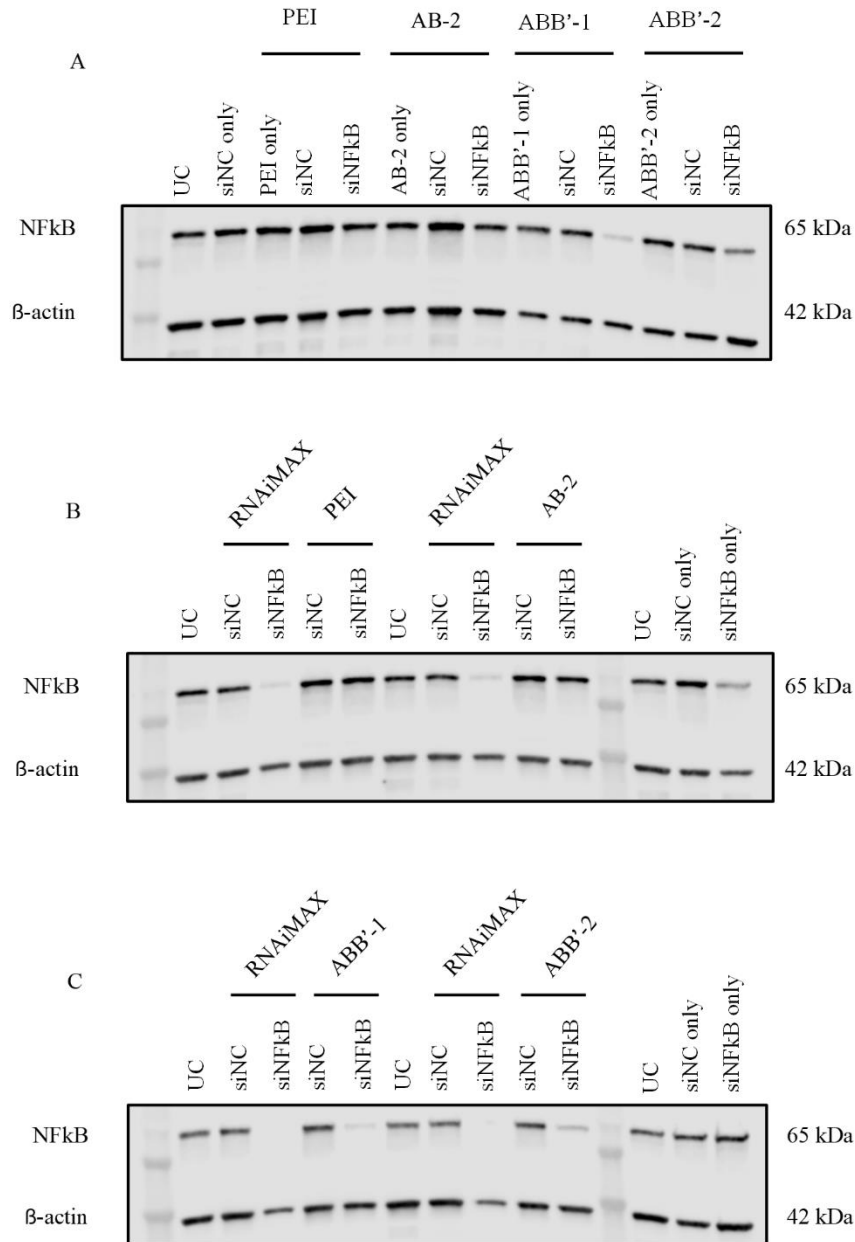


Figure S42: Western blot analysis of in vitro gene silencing efficacy of NFκB (p65) in MIO-M1 cell line transfected with polymers/siRNA polyplexes at an N/P ratio of 5 in comparison to commercialized transfection reagent RNAiMAX. Untreated MIO-M1 was included as control (UC). Cells treated with Silencer™ negative control siRNA (siNC) or siRNA targeting NFκB (siNFκB) were evaluated to rule out its potential knockdown effect. **(A)** MIO-M1 treated with respective polymer only at the same concentrations were included and showed no effects on NFκB (p65) knockdown. **(B)** Cells transfected with PEI/siNFκB or AB-2/siNFκB do not show apparent knockdown of NFκB expression. **(C)** Superior NFκB (p65) gene silencing efficacy was observed in cells transfected with ABB'-1/siNFκB or ABB'-2/siNFκB when in comparison to that of PEI/siNFκB or AB-2/siNFκB.

Table S3: Primary antibody source and dilution.

Antibody Target	Source	Dilution
NFκB p65	Ms monoclonal, Elabscience (E-AB-22016)	1:500
β-actin	Rb monoclonal, Cell Signaling (13E5)	1:1000

### 13) References

- (1) Salzinger, S.; Soller, B. S.; Plikhta, A.; Seemann, U. B.; Herdtweck, E.; Rieger, B. Mechanistic studies on initiation and propagation of rare earth metal-mediated group transfer polymerization of vinylphosphonates. *J. Am. Chem. Soc.* **2013**, *135* (35), 13030–13040. DOI: 10.1021/ja404457f.
- (2) Leute, M. Macromolecules with Phosphorus. Dissertation, Universitat Ulm, Ulm, 2007.
- (3) Schwarzenböck, C.; Nelson, P. J.; Huss, R.; Rieger, B. Synthesis of next generation dual-responsive cross-linked nanoparticles and their application to anti-cancer drug delivery. *Nanoscale* **2018**, *10* (34), 16062–16068. DOI: 10.1039/C8NR04760J.
- (4) Hartl, N.; Adams, F.; Costabile, G.; Isert, L.; Döblinger, M.; Xiao, X.; Liu, R.; Merkel, O. M. The Impact of Nylon-3 Copolymer Composition on the Efficiency of siRNA Delivery to Glioblastoma Cells. *Nanomaterials* **2019**, *9* (7). DOI: 10.3390/nano9070986. Published Online: Jul. 8, 2019.
- (5) Adams, F.; Zimmermann, C. M.; Baldassi, D.; Pehl, T. M.; Weingarten, P.; Kachel, I.; Kränzlein, M.; Jürgens, D. C.; Braubach, P.; Alexopoulos, I.; Wygrecka, M.; Merkel, O. M. Pulmonary siRNA Delivery with Sophisticated Amphiphilic Poly(Spermine Acrylamides) for the Treatment of Lung Fibrosis. *Small* **2023**, e2308775. DOI: 10.1002/sml.202308775. Published Online: Dec. 21, 2023.
- (6) Wu, S.; Liang, F.; Hu, D.; Li, H.; Yang, W.; Zhu, Q. Determining the Critical Micelle Concentration of Surfactants by a Simple and Fast Titration Method. *Anal. Chem.* **2020**, *92* (6), 4259–4265. DOI: 10.1021/acs.analchem.9b04638. Published Online: Feb. 26, 2020.
- (7) G. Astrid Limb; Thomas E. Salt; Peter M. G. Munro; Stephen E. Moss; Peng T. Khaw. In Vitro Characterization of a Spontaneously Immortalized Human Müller Cell Line (MIO-M1). *Invest. Ophthalmol. Vis. Sci.* **2002**, *43* (3), 864–869.

- (8) Schnichels, S.; Hagemann, U.; Januschowski, K.; Hofmann, J.; Bartz-Schmidt, K.-U.; Szurman, P.; Spitzer, M. S.; Aisenbrey, S. Comparative toxicity and proliferation testing of aflibercept, bevacizumab and ranibizumab on different ocular cells. *Br. J. Ophthalmol.* **2013**, *97* (7), 917–923. DOI: 10.1136/bjophthalmol-2013-303130. Published Online: May. 17, 2013.
- (9) Fietz, A.; Hurst, J.; Schnichels, S. Out of the Shadow: Blue Light Exposure Induces Apoptosis in Müller Cells. *Int. J. Mol. Sci.* **2022**, *23* (23). DOI: 10.3390/ijms232314540. Published Online: Nov. 22, 2022.
- (10) Hausig-Punke, F.; Richter, F.; Hoernke, M.; Brendel, J. C.; Traeger, A. Tracking the Endosomal Escape: A Closer Look at Calcein and Related Reporters. *Macromol. Biosci.* **2022**, *22* (10), e2200167. DOI: 10.1002/mabi.202200167. Published Online: Aug. 17, 2022.
- (11) Lai, J. C.; Rounsfell, T.; Pittman, C. U. Free-radical homopolymerization and copolymerization of vinylferrocene. *J. Polym. Sci. A-1 Polym. Chem.* **1971**, *9* (3), 651–662. DOI: 10.1002/pol.1971.150090307.
- (12) Fineman, M.; Ross, S. D. Linear method for determining monomer reactivity ratios in copolymerization. *J. Polym. Sci.* **1950**, *5* (2), 259–262. DOI: 10.1002/pol.1950.120050210.